coatings

MDPI

Review

Excitation Threshold Reduction Techniques for Organic Semiconductor Lasers: A Review

Yao Wang [1], Xu Han [1], Linze Jin [1], Yuhui Meng [1], Chengming Jiang [1], Kyeiwaa Asare-Yeboah [2], Zhengran He [2,*] and Sheng Bi [1,*]

[1] Key Laboratory for Precision and Non-Traditional Machining Technology of the Ministry of Education, Dalian University of Technology, Dalian 116024, China
[2] Department of Electrical and Computer Engineering, Penn State Behrend, Erie, PA 16563, USA
* Correspondence: zmh5222@psu.edu (Z.H.); bish@dlut.edu.cn (S.B.)

Abstract: Organic semiconductor lasers have shown great application potential in various fields, such as low-cost sensing, high-performance lighting and display, and lab-on-a-chip devices. Since the introduction of organic lasers in the 1960s, research on semiconductor laser devices has expanded to include various materials and structures. The organic laser has attracted much attention due to its wide range of emission spectrum and simple synthesis and processing. Researchers constantly pursue the goal of using organic semiconductors to fabricate low-threshold thin-film organic laser devices while retaining the characteristics of a wide luminescence spectrum of organic materials, simple and portable structure, and low cost. However, organic semiconductor lasers face challenges due to material stability under optical pumping and large optical losses under electrical pumping, making commercialization difficult. Many scholars have put great efforts into enhancing the performance of materials and optimizing the structure to minimize the threshold of organic semiconductor lasers. Herein, based on the basic principles of organic lasers, the main factors affecting the excitation threshold are summarized. A comprehensive analysis of the relevant factors and threshold conditions is performed, considering both positive and negative aspects of modal gain and modal loss that need to be addressed. We expect to provide a wide range of ideas for reducing the threshold of organic lasers and offer theoretical guidance for the practical industrial production of organic lasers.

Keywords: organic semiconductor lasers (OSLs); excitation threshold; exciton annihilation; optical feedback; structural design

check for updates

Citation: Wang, Y.; Han, X.; Jin, L.; Meng, Y.; Jiang, C.; Asare-Yeboah, K.; He, Z.; Bi, S. Excitation Threshold Reduction Techniques for Organic Semiconductor Lasers: A Review. *Coatings* **2023**, *13*, 1815. https://doi.org/10.3390/coatings13101815

Academic Editor: Angela De Bonis

Received: 5 August 2023
Revised: 26 September 2023
Accepted: 11 October 2023
Published: 23 October 2023

Copyright: © 2023 by the authors. Licensee MDPI, Basel, Switzerland. This article is an open access article distributed under the terms and conditions of the Creative Commons Attribution (CC BY) license (https://creativecommons.org/licenses/by/4.0/).

1. Introduction

In the 1960s, organic materials were used for laser gain material [1]. Its history almost coincides with that of the laser itself. Additionally, the functional properties, as well as the performance of these laser devices, have undergone considerable development and improvement, especially with continuous breakthroughs in semiconductor theory, materials, and preparation technology. Organic semiconductor materials form laser materials with important prospective applications because of their unique optoelectronic characteristics, such as simple synthesis and processing, and the functionalized design of their molecular structure [2,3]. In addition, organic lasers have the advantages of simple preparation technology, low cost, large area preparation, and easy integration. These are the special characteristics that traditional crystal lasers and laser diodes cannot achieve. The rapid development of organic semiconductor lasers has enriched the field of laser technology, leading to potential applications in low-cost sensing, high-performance lighting and display, optical communication, and lab-on-a-chip (LoC) devices [4–7]. Since the formation of the optically pumped organic solid-state laser (OSSL) developed on conjugated polymers in 1996 [8,9], the optically pumped organic semiconductor laser has performed excellently in both solution and solid states, serving as a conjugate polymer laser or host-guest doped

organic small molecule laser. Now, the realization of the electrically pumped organic semiconductor laser has become a central focus within the discipline of organic optoelectronics. Researchers have found that the current optically pumped OSSL exhibits a narrow half-width (only 0.01 nm) [10] with a high peak output power evolved from the long-wavelength side of the transverse electric TE stop band, as well as a wide coverage of stimulated emission spectrum. The laser wavelength of optically pumped organic semiconductor lasers encompasses the entire visible spectrum.

The continuous generation of lasers must satisfy three conditions: population inversion, a threshold requirement, and a resonance condition. Irradiation of energy (excitation light) to the laser medium from the outside causes a large number of atoms to jump from a low energy ground state (E_1) to a specific excited state (E_3), resulting in stimulated radiation that dominates and releases photons with specific energy. After reaching the threshold requirement, photons are continuously generated and amplified 10~1000 times in the resonant cavity to form a laser of a specific wavelength. Therefore, population inversion and the threshold condition are necessary but not sufficient. In order to advance these two prerequisites, scholars have continuously explored and innovated in materials, structure, and preparation techniques [2]. Many remarkable achievements in the innovation of organic laser devices have been made (Figure 1). A more advanced doping system with high gain, comprehensive design, and construction of the micro-cavity structure with low loss and high Q value has also been created to continuously reduce excitation threshold conditions and make lasers easier to realize. Thus, they pave the way for practical applications of organic laser devices.

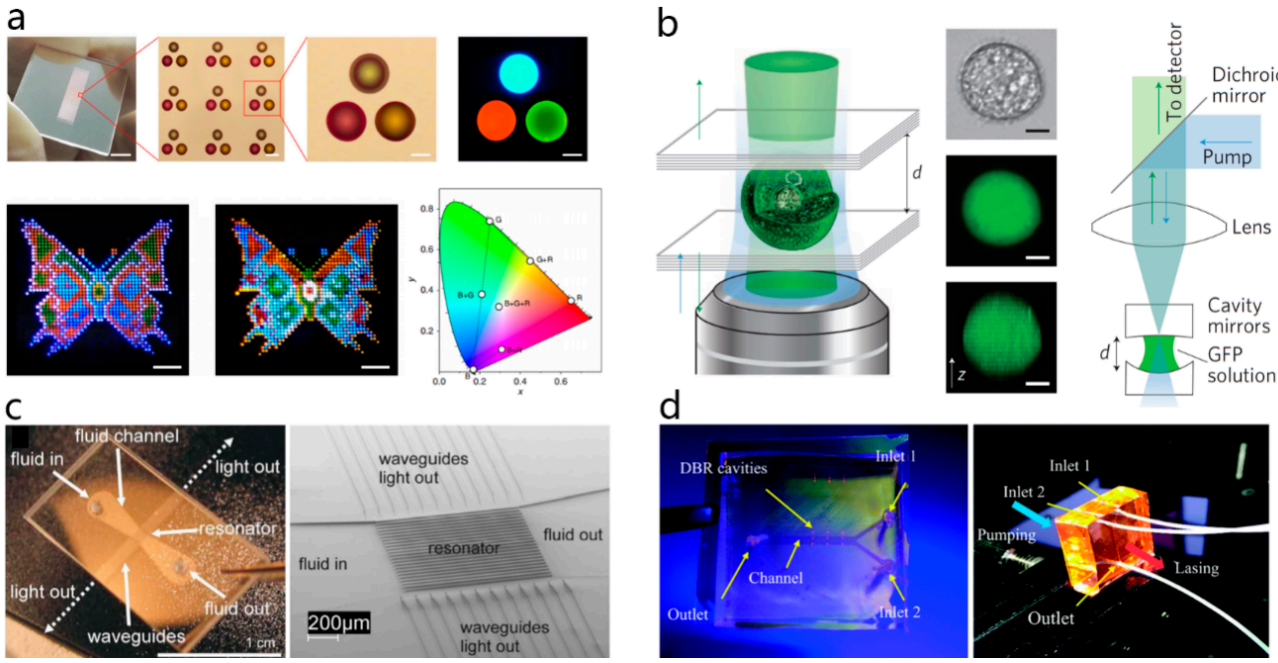


Figure 1. Several frontier applications of organic lasers. (**a**) Full-color optically pumped organic solid-state laser displays [4]. Copyright 2019 Nature Communications (**b**) The biological cell laser based on green fluorescent protein (GFP) that may be used for intracellular sensing, cytometry, and imaging [5]. Copyright 2011 Nature Photonics (**c**) The LoC device with integrated microfluidic channel, optical microcavity, and output coupling waveguides [6]. Copyright 2005 Optoelectronic Integration on Silicon II (**d**) Microfluidic channels combined with organic distributed Bragg reflector lasers for field sensing applications [7]. Copyright 2018 Journal of Materials Chemistry C.

In this review, we generally discuss the development and research status of organic lasers, and we mainly introduce the new progress in this field. However, the core problem of organic lasers—methods of threshold reduction—has not been systematically sorted out and elaborated. Based on the basic principle of organic lasers, we summarize the

main conditions affecting the excitation threshold in this review. From these aspects, we introduce the methods of reducing the excitation threshold in terms of material and structure. Moreover, we emphatically introduce the method of threshold reduction for electrically pumped organic semiconductor lasers in a different way than that of optically pumped lasers. Finally, we summarize the methods introduced in this review and provide a prospect for the future of organic lasers. We hope this review will be useful to researchers engaged in the research of organic laser devices.

2. Basic Theory of Excitation Threshold Reduction in Organic Semiconductor Lasers

2.1. The Building Blocks of Lasers

An organic semiconductor laser device usually refers to the structure and processing of organic optoelectronic devices. These are low-cost devices that consist of a pumping source, a laser medium, and an optical feedback layout to induce particles from the ground state to higher energy levels in order to achieve population inversion. They are totally divided into different types of excitations, including optical excitation, gas discharge excitation, electrical excitation, and nuclear excitation, depending on the state of the gain material. To achieve population inversion, quasi-four-level materials are chosen as the laser medium, including gas, liquid, solid, and semiconductor. Optical feedback layout is utilized to increase the effective length of the working medium and determine the output characteristics of the laser, such as monochromaticity, directionality, and coherence.

In general, organic semiconductor lasers can be simplified to a structure with organic semiconductor materials as the intermediate gain media and two mirrors as the light feedback structures (Figure 2). One of the mirrors is a semi-transparent mirror (95% reflectivity). If the pump sources provide energy above the threshold requirement to generate a large number of particles in the excited state of the gain medium organic material, thus achieving population inversion, and if a portion of the light emitted spontaneously by the gain medium hits the mirror vertically, it enables a back-and-forth reflection between the mirror and the semi-transparent mirror, repeatedly traversing the organic gain medium during this process. Furthermore, the light can trigger the gain material to produce stimulated emission instead of spontaneous emission consecutively, thus achieving amplification. If the total gain of the pumping source equals or exceeds the loss caused by incomplete reflection and absorption of the mirror, as well as the absorption in the organic material during the reflection process, a continuous laser emission can be maintained. After abundant diffraction and amplification in the optical resonant cavity, coherent light that is perpendicular to the axis of the resonant cavity is emitted from the semi-transparent mirror, forming the laser eventually.

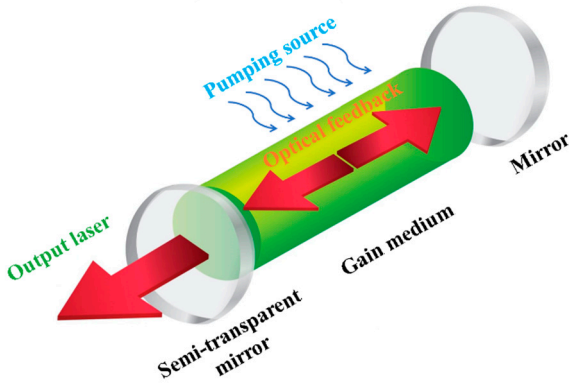


Figure 2. Organic laser structure: a pumping source, a mirror, a semi-transparent mirror, and a gain medium.

2.2. Quasi Four-Level Laser Structure of Organic Semiconductors

In order to realize population inversion, the material must have a metastable level. Due to the fact that the rate of stimulated emission equals light absorption in thermal

equilibrium, the number of particles at the higher energy level must be less than at the lower energy level. As a result, the material of a two-level system cannot achieve population inversion. Comparatively, with traditional laser materials, the organic gain material possesses a three or quasi-four-level distribution. This allows the excitation to stay in the excited state steadily, making population inversion easily achievable when excited—A necessary condition for obtaining a laser. Unlike the three-energy level system, it is easier to achieve population inversion between energy levels E_2 and E_3 since the number of particles in the sub-stable energy level E_2 is lower. This results in a decline of the excitation threshold (Figure 3). Thus, organic crystals, organic small molecules, and conjugated polymers with a four-level system are usually chosen as the gain medium. In organic semiconductor lasers with different materials and structures, many measures are taken to reduce the excitation threshold, which is a comprehensive result of multiple conditions, such as modal gain and absorption. To illustrate these methods more systematically, gain, loss, and Q factor are introduced to describe the conditions of continuous laser emission in a more intuitive manner.

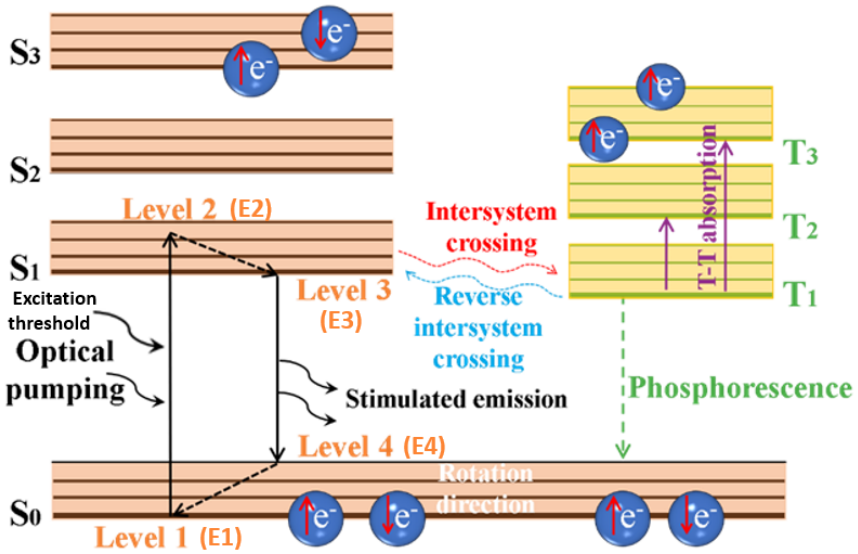


Figure 3. Schematic diagram of typical four-energy-level system of organic laser materials, representing singlet excitons, triplet excitons.

2.3. Optical Feedback Structure

As one part of the organic laser device, the configuration of the microcavity can influence the performance of organic lasers by adjusting its size or changing its type. Typical optical microcavities include Fabry–Pérot microcavities, distributed Bragg reflector structures (DBR), whispering gallery mode resonators (WGM), and distributed feedback structures (DFB).

The continuous emission of light in an organic laser can be understood as an increase in intensity rather than a decrease as it passes through the gain medium between the two reflective surfaces. In other words, the modal gain must be equal to or exceed the losses existing in the structure for the device to achieve excitation conditions. The Q factor is necessary to describe the ability of the optical feedback structure to retain light.

According to the excited emission theory, when the gain medium in the excited state interacts with an incident photon, it releases an additional photon with the same direction and frequency as the incident photon, leading to light amplification and modal gain. This phenomenon corresponds to the particle density in the excited state within the gain medium in a significant manner. Additionally, the particle density in the excited state is highly dependent on the pump strength, determining the excitation threshold, which is the minimum pumping strength required for modal gain to exceed modal loss.

To reduce the excitation threshold, both aspects need to be examined. Regarding modal gain, its magnitude is not only related to the pump strength but fundamentally depends on the basic properties of the gain medium itself. Exploring materials and different doping processes that can achieve population inversion at lower pumping strength is an efficient technique used to increase modal gain and minimize the threshold of laser excitation in the organic semiconductor.

The resonant cavity parameters directly affect the density of emitted photons, thereby influencing both the laser threshold and slope efficiency. By increasing the Q factor from 2000 to 4000 [11], the cavity loss and laser threshold decrease due to the rise in photon lifetime and excitation generation within the cavity. On the other hand, constructing a high-Q microcavity structure that continuously reduces mode loss is another effective way to decrease the excitation threshold.

2.4. Excitonic and Photonic Losses

Recently, remarkable improvements in the performance of Organic Semiconductor Lasers (OSLs) have been achieved in parallel with the development of Organic Light Emitting Diodes (OLEDs). State-of-the-art OLED materials and device architectures provide the foundation for OSLs and OSLDs (Organic Semiconductor Laser Diode). However, operating OSLs under the continuous-wave (CW) regime and electrical excitation with a low current threshold remains a significant challenge due to various loss mechanisms, such as excitonic annihilations, excited-state absorptions, and cavity losses that hinder their operation. In accordance with the law of conservation of energy, reducing system losses is an effective way to increase efficiency while maintaining constant input gain. By decreasing overall excitonic and photonic losses, the threshold decreases, and the slope efficiency increases.

Organic semiconductor lasers can be divided into two types: optically pumped organic lasers and electrically pumped organic lasers, based on the variation in pumping modes. These two types of laser devices exhibit significant differences in theory, structure, and methods employed to reach the excitation threshold conditions. Therefore, they should be presented separately.

The various loss mechanisms in OSLs and OSLDs, which contribute to an increase in the laser threshold and a decrease in the slope efficiency, can be categorized into excitonic loss and photonic loss mechanisms, as shown in Figure 4. Excitonic losses quench the excitons in an active layer and include singlet-singlet annihilation (SSA), singlet-triplet annihilation (STA), singlet-polaron annihilation (SPA), singlet exciton dissociation by an external electric field, and exciton quenching at the interface of a metallic electrode (Figure 3). On the other hand, photonic losses, which annihilate emitted photons, consist of cavity losses, such as the absorption of photons by singlet and triplet excitons [11], as well as polarons and the absorption by electrodes. The singlet and triplet absorptions (TAs) are quantified by singlet and TA cross-sections, which indicate the probability of interaction between photons and excitons in each excitonic state.

After comprehensive analysis, it is found that the laser threshold decreases significantly with STA, SSA, and SPA declining as 75% of triplet excitations of total excitations are forced to generate directly from electron-hole recombination, leading to a reduction in photon density. Among them, SPA is the most critical excitation loss mechanism in electrical excitation. In contrast, TTA can decrease the laser threshold by reducing the density of triplet excitations (transition mechanism can be seen in Table 1). Long-lived triplet excitons generally cause the absorption of emitted photons, inducing significant optical losses for light amplification. This loss mechanism is noticeable when the excited state absorption and the emission spectra overlap. These reabsorption losses are important mechanisms that affect the laser threshold and slope efficiency. Additionally, reducing the production and annihilation of triplet excitons and harvesting the triplet excitations by utilizing thermally activated delayed fluorescence (TADF) emitters or phosphorescence

can achieve light amplification and efficiency enhancement, opening up a novel guideline aimed at realizing an OSLD.

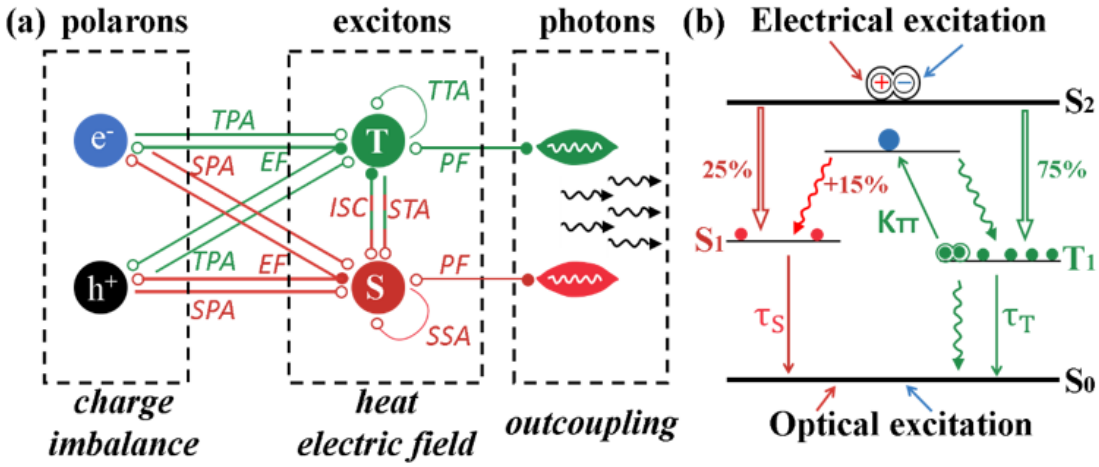


Figure 4. (**a**) Diagram of typical annihilation of organic laser materials [11]. (**b**) The comparison between electrical excitation and optical excitation. Copyright 2017 Canadian Journal of Chemistry.

Table 1. Transition mechanisms in an organic laser gain medium [12].

Mechanism	Reaction Formula	Optical Excitation	Electnical Excitation
Inter-system crossing (ISC)	$S_1 \overset{K_{ISC}}{\rightarrow} T(1)$	√	√
Reverse inter.syslem crossing (RISC)	$T_1 \overset{K_{RISC}}{\rightarrow} S_1(2)$	√	√
Singlet-triplet annihilation (STA)	$S_1 + T_1 \overset{K_{STA}}{\rightarrow} T_1 + S_0(3)$	√	√
Singlet-singlet annihilation (SSA)	$S_1 + S_1 \overset{(1-g)K_{SSA}}{\rightarrow} T(1) + S_0(4)$	√	√
Triplet.triplet annihilation (TTA)	$S_1 + S_1 \overset{RK_{SSA}}{\rightarrow} S_1 + S_0$ $T_1 + T_1 \overset{(1-g)K_{TTA}}{\rightarrow} T_1 + S_0(5)$	√	√
Singlet-polaron annihilation (SPA)	$T_1 + T_1 \overset{gK_{TTA}}{\rightarrow} S_1 + S_0$ $S_2 + \text{polaron} \overset{K_{SPA}}{\rightarrow} S_0 + \text{polaron}(6)$	×	√
Triplet.polaron annihilation (TPA)	$T_1 + \text{polaron} \overset{K_{PTA}}{\rightarrow} S_0 + \text{polaron}(7)$	×	√
Singlet absorption (SA)	$S_1 + \text{polaron} \overset{\sigma_g}{\rightarrow} S_n(8)$	√	√
Triplet absorption (TA)	$T_1 + \text{polaron} \overset{\sigma_t}{\rightarrow} T_n(9)$	√	√

3. Measures of Threshold Reduction of Optically Pumped Organic Laser in Terms of Materials

Commonly used organic molecules in organic semiconductor lasers possess Stokes shifts that are very evident due to vibrational relaxation during the excitation/emission event. The luminescence spectrum shifts more towards lower energy compared to the absorption spectrum, resulting in organic molecules having a small absorption coefficient for their own fluorescence. This leads to high absorption for excitation light (absorption coefficient > 1×10^5 cm^{-1}). Consequently, the low absorption at the laser's wavelength can be easily separated, defining the characteristics of the device. It can be excited when the modal gain is relatively low, which means the Stokes shift greatly reduces the excitation threshold [13–15]. Due to the amorphous conformational distribution of the π-conjugated organic molecules commonly used in organic semiconductor laser devices, the energy level distribution of different molecular segments is very wide. Rudenko et al. used the Gaussian disorder model to explain the phenomenon where light excited at different energy positions of the material quickly transfers to the lowest energy molecules or molecular fragments after absorption. Thus, the laser emission consistently occurs between the zero-level state

and the lowest excited state energy, with the emission spectrum of the gain medium relative to the red shift of the absorption spectrum [16,17]. Almost all of the light is absorbed by the wide band gap of the organic material, and the modal loss is substantially reduced after several emission and absorption processes, effectively lowering the excitation threshold with constant gain. The energy transfer characteristics of organic molecules enable materials with different energy gaps to form a mixed gain medium system through doping and other means. High-energy gap organic semiconductor materials absorb pumping energy and consequently achieve low threshold laser emission by coupling between excitation and emission light to increase the Stokes shift [18,19].

In organic semiconductor laser devices, there are parasitic effects on the laser emission wavelength, mainly from the absorption in the triplet state, which affect the laser emission and can raise the excitation threshold or even completely stop the laser emission [20,21]. When the organic gain medium is in the excited state S_1 under the stimulation of the pumping source, it tends to relax back to the ground state S_0. However, there is also a small possibility of accessing the first triplet state T_1 through intersystem crossing. Although the emission intensity of the triplet exciton in the system is very weak, its lifetime is usually very long because its spin is prohibited from returning to the S_0 ground state. As a result, the energy is only released in the form of heat slowly instead of rapid excitation emission. Furthermore, the organic material may also change its spin direction through the intersystem channel or heat release, transitioning to the higher excited state Tn by energy absorption and annihilation. In this process, the absorption spectrum of the excited state tends to overlap with the emission spectrum of organic materials, greatly increasing the modal loss and raising the threshold accordingly. Even the triplet excitons accumulate over time and result in the laser device being able to run for only a few nanoseconds [10,22]. This adversely affects the continuous operation of organic lasers. Therefore, suppressing the triplet excitons to diminish the threshold and guarantee continuous operation of the device is of great importance.

In organic lasers, organic dyes and fluorescent organic semiconductor materials account for almost all the gain medium materials, and they share many commonalities. However, as organic lasers extend to electric pumping, the semiconductor properties of the gain medium become particularly important. For example, Samuel and Turnbull regard the ability of organic semiconductors to transmit carriers as an important basis for distinguishing them from organic dyes [23]. In their paper, organic materials were classified into organic dyes, organic semiconductors, and other new materials according to their three standards: processability in thin film manufacturing, high fluorescence quantum yield (PLQY) even in neat films, and charge transfer capability. A plethora of scholars have applied new materials and innovated the doping process, allowing the gain medium to experience a large Stokes shift, greatly reduced modal loss, avoidance of the triplet state effect, and significant diminishment of the excitation threshold value.

3.1. Organic Dyes

Organic dyes are the earliest materials used as laser gain media. Their most primitive form involves dissolved dye molecules in liquid solvents, functioning as the gain media. To prevent the triplet accumulation of organic dye molecules and ensure the continuous operation of the laser, the organic dye solution is usually cycled through the optical cavity. However, this method makes the use of devices extremely complex and raises serious safety concerns, making it completely unsuitable for meeting the convenience requirements of organic semiconductors. Instead, an effective method to develop the organic solid laser is by doping dyes into a solid matrix or using molecular glass and film [24,25]. Currently, the main employed organic dye series include Coumarins, Xanthenes, and Pyrromethenes (Figure 5).

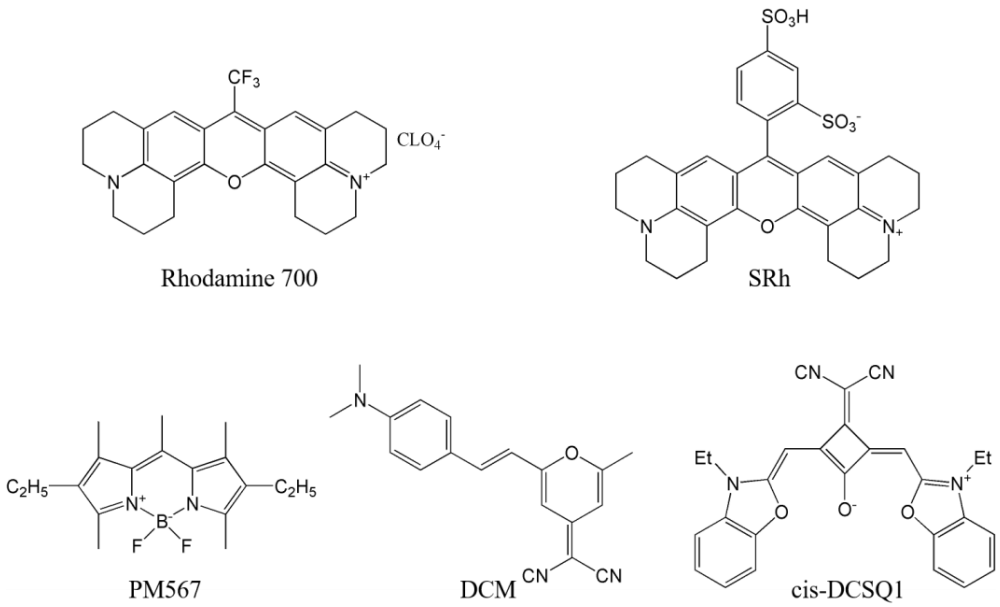


Figure 5. Molecular structures of several organic dyes, Rhodamine 700, SRh, PM567, DCM, cis-DCSQ1.

Polymethyl methacrylate (PMMA) is a widely used semiconductor device in the matrix. Wallikewitz constructed an active layer of (0.8 ± 0.1) µm. The structure was fabricated by rotating a chloroform solution containing 1% laser dye, 20% spiropyran (10,30-dihydro-10,30,30-trimethyl-6-nitrospiro [2H-1-benzopyran-2,20-(2H)-indole]), and 79% PMMA. The DFB laser, fabricated using nanoimprint lithography, exhibited a low laser threshold of 50 µJ·cm^{-2} [26]. Zhou et al. prepared salmon deoxyribonucleic acid (DNA) films with surfactants acting as the host of the laser dye sulforhodamine (SRh) [27]. The DNA film has an absorption peak at 260 nm, while the SRh molecule has an absorption peak at 578 nm and an emission peak at 602 nm, resulting from the absorption of aromatic nitrogenous bases. Consequently, the PMMA:SRh grating achieved a 50% excitation pump energy threshold using this method, with the SRh molecular emission peak separated from the DNA film and as low as 3 µJ.

Liu et al. blended two different dyes, leading to a significantly reduced threshold of the dye-doped holographic polymer dispersed liquid crystal gratings DFB laser. The dyes were prepared by utilizing a two-dimensional photonic crystal guest and a guest-host system [28]. The guest emitter 4-(dicyanomethylene)-2-methyl-6-(4-dimethylaminostyryl)-4H-pyran (DCM) with various doping concentrations in the main dye 1,3,5,7,8-pentamethyl-2,6-diethylpyrromethene-difluoroborate (PM567) was incorporated into the holographic polymer dispersed liquid crystal (HPDLC) transmission grating. The DFB laser can be discerned in intrinsic host, intrinsic guest, and guest-host (G-H) systems. Utilizing the effective Förster energy transfer, the self-absorption of the laser wavelength was significantly inhibited, and the laser threshold was reduced to 1.35 µJ/Pulse, far below the threshold without the energy transfer process. Organic dyes were doped into organic semiconductor materials to construct a G-H system. Hence, by physically separating the emission unit and transferring the effective energy to low energy gap organic dyes through the Förster energy transfer, the emission and absorption peaks of the gain medium could be significantly separated, eliminating the concentration quenching of organic dyes and reducing the excitation threshold [29,30]. For example, if a doping system is constructed with Alq3 as the host and DCM as the host, the host material with the high band gap, Alq3, will absorb pump energy, subsequently transferring its energy to the host, DCM, with the low energy gap through the Förster energy transfer. A large Stokes displacement will decrease the mode loss, and the laser threshold will be reduced accordingly [15,30].

Ye et al. reported a cis-DCSQ1 deep red amplified spontaneous emission (ASE) with a cis-configuration (cis-DCSQ1) under an optical pump [31]. They prepared the

film by doping cis-DCSQ1 into a 4,4′-bis(9-carbazolyl)-2,2′-biphenyl (CBP) material at a concentration of 0.5 wt%. Owing to the self-absorption and increased photoluminescence quantum efficiency due to the reduction of chromophore-chromophore interaction of polymerization caused by the effective CBP-to-cis-DCSQ1 Förster resonance energy transfer and quenching, the photoluminescence quantum yield of films with CBP as the main body is immensely increased by an appropriate concentration. The doped membrane had an ASE threshold of about 10 $\mu J \cdot cm^{-2}$ and a 687 nm emission peak. These results prove that cis-configured squaraine derivatives are promising as gain materials for future applications as deep-red organic lasers.

For organic dyes, when they are doped into polymer hosts, such as Polystyrene (PS), Polymethyl methacrylate (PMMA), or Polyvinyl carbazole (PVK), organic semiconductor devices can be fabricated using the spin-coating method or the vacuum-deposited method directly on flexible substrates to ensure uniformity. Thanks to the flexibility of their chemical structure, organic dyes can alter the effective conjugation length or distribution of the π-orbitals on the molecule or within a block. As a result, the dipole distance of the excited state of the material increases, along with the Stokes shift, which effectively inhibits triplet absorption, reduces the excitation threshold and ensures laser operation.

3.2. Organic Semiconductor Materials

The field of organic semiconductor studies has rapidly developed in terms of materials and preparation techniques since they were first used in the light-emitting layer of organic spontaneous photodiodes in the late 1980s [32]. Researchers have also gained a deeper understanding of the properties of the materials and their luminescence principles, as well as their optoelectronic characteristics. These properties allow the materials to be applied as organic solid-state lasers. By adopting the appropriate doping process and modification methods, the mode loss can be reduced, and triplet quenching can be achieved, making it possible to use OSSL with a low threshold. Moreover, the greatest strength of organic semiconductors over organic dyes lies in their charge transfer performance. Although the carrier mobility of organic semiconductors is significantly lower than that of inorganic semiconductors, it also offers the possibility of electrically pumping organic semiconductor lasers. The organic semiconductor materials used in organic lasers mostly comprise organic crystals, small organic molecules, dendritic starburst molecules, and conjugated polymers, among others.

3.2.1. Organic Crystals

Organic crystals exhibit anisotropy and possess excellent crystal structures. Due to their capacity to form self-excited cavities, they offer unique advantages as gain media in semiconductor lasers. Moreover, organic crystals usually have higher refractive indices and polarization emissions, which are beneficial for enhancing light reflection, reducing modal loss, and lowering excitation thresholds. The performance of the gain medium in organic crystals is greatly influenced by molecular stacking, crystal quality, and intermolecular interactions.

In 2003, Wu et al. [33] prepared a high-quality single crystal of distyrylbenzene (DSB) from the gas phase, studied its structure and optical properties, and determined that its crystal structure was orthorhombic. Low-temperature photoluminescence (PL) emission revealed abundant vibronic substructures with high PL quantum yield, exhibiting self-waveguide-induced laser action at room temperature. To improve the performance, inhibit fluorescence quenching, and reduce the excitation threshold, various distyrylbenzene derivatives with different substituents were constructed in comparison to phenylenevinylene. Effective methods included replacing benzene with alkoxy- and alkyl-flexible chains or altering the position of benzene in DSB phenyl units [34–36].

Kabe et al. [37] prepared simplified diphenyl derivatives, namely, 1,4-bis(4-methylstyryl) benzene (p-MSB) and 1,4-bis(2-methylstyryl)benzene (o-MSB). An ultra-low amplified spontaneous emission (ASE) threshold of 14 $\mu J \cdot cm^{-2}$ was obtained from the o-MSB single crystal

(Figure 6), which was much lower than that of DSB. The single crystal of the distyrylbenzene derivative exhibited a low excitation threshold, excellent charge carrier transport characteristics, and high fluorescence quantum efficiency. The development of current-driven organic lasers with organic crystals as the gain medium is an important field for future research.



Figure 6. Molecular structures of DSB, p-MSB, and o-MSB.

3.2.2. Small Organic Molecules

Organic small-molecule semiconductors are commonly used as organic materials to develop organic light-emitting diodes (OLEDs). They have small molecular weights, and most films are prepared through hot evaporation. The π-π stacking among small organic molecules and the dipole interactions among their units eventually lead to intrinsic fluorescence quenching. This reduction in modal gain increases the excitation threshold. Scholars have tried various methods in molecular design to improve the optical emission performance of thin films. Some of these methods include constructing a D-π-A structure using branch chain functions and strictly spatial requirement substitution to reduce the quenching effect of organic small molecular gain medium and to minimize the adverse effect of intermolecular π-π stacking on organic lasers [38–40]. Fluorene is a common fluorescent structural group that can easily form functional groups and solubilized groups through cross-coupling reactions. This allows the production of various molecules based on fluorene (Figure 7). Choi et al. [41] studied the photophysical properties and ASE properties of a series of oligomer fluorene treated with monodisperse solutions, functionalized by a hexyl chain at the C_9 position of different fluorene units. The fluorene positions functionally developed linear oligomer fluorene of hexyl chains, and an ASE threshold of 0.4 μJ·cm^{-2} was obtained in a nitrogen environment.

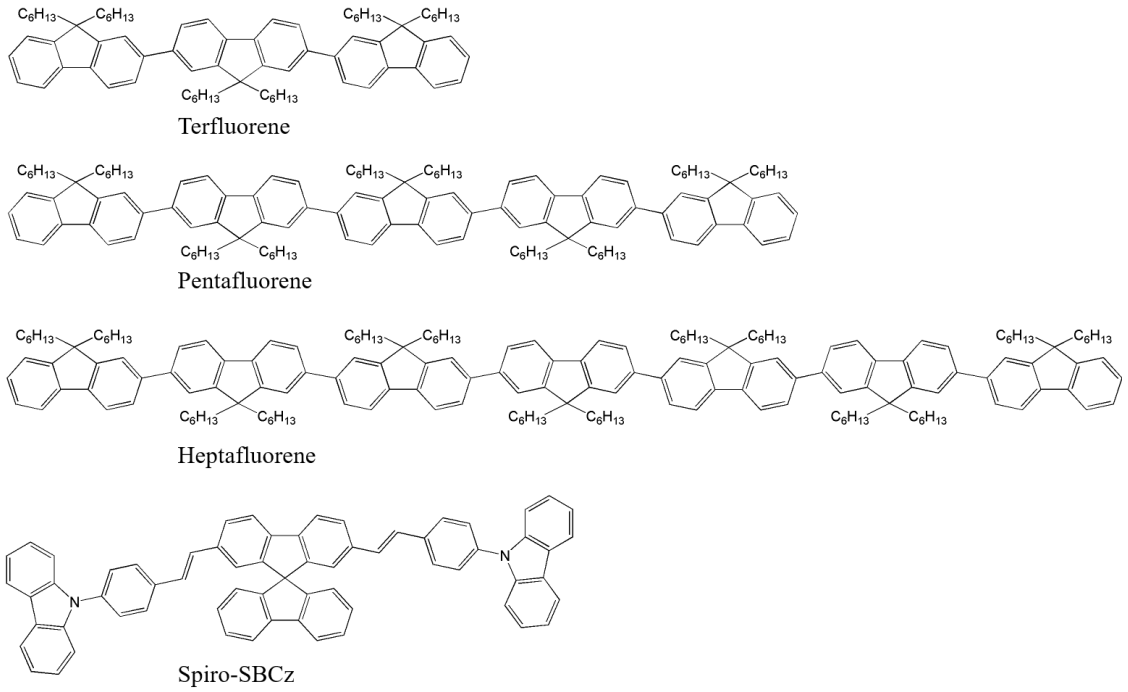


Figure 7. Molecular structures of several small organic molecules.

Sandanayaka et al. [42] constructed a DFB laser using a mixture of liquid 9-(2-ethylhexyl) carbazole matrix doped with the heptafluorene derivative as the gain medium. The effects of molecular oxygen and other triple quenchers on the quasi-continuous wave laser characteristics were studied by adding oxygen or nitrogen into the liquid gain medium. The threshold value of the oxygenated laser device was 2 $\mu J \cdot cm^{-2}$, which was below the value of the nitride laser and was not affected by the repetition frequency in the range of 0.01~4 MHz.

Nakanotani et al. [43] doped 2,7-bis [4-(N-carbazole)phenylvinyl]-9,9′-spirobifluorene (spiro-SBCz) into the broad bandgap 4,4′-bis(9-carbazole)-2,2′-biphenyl (CBP) host to achieve the low ASE threshold of E-th = 197 $nJ \cdot cm^{-2}$, which is the lowest threshold thus far. Moreover [44], the spiro-SBCz film was confirmed to play the role of an active light-emitting layer in an OLED and a field-effect transistor (FET). Linear electroluminescence in FET structures was successfully obtained, which is of great significance for future organic laser diodes.

3.2.3. Dendritic Starburst Molecules

Dendrimers and star-shaped macromolecules usually consist of a central core and numerous functional π-conjugated arms. They are a type of organic material that combines the morphological characteristics of polymers with properties similar to small molecules, resulting in excellent optoelectronic properties [45–47]. The inhibition of aggregation and self-quenching arises from the highly branched projections of dendritic starburst molecules, which significantly reduce their modal losses. Moreover, their unique structure has the potential to synthesize large structures and complex branching materials, leading to lower excitation thresholds and improved laser properties.

Lawrence et al. [48] investigated the ASE characteristics of three types of bisfluorene-cored dendrimers in solids. Their study demonstrated that the dendron types have a significant influence on the ASE threshold, optical gain, loss coefficient, and photoluminescence quantum yield (Figure 8). To form dendritic starburst molecules, they attached biphenylcarbazole (BPCz), biphenyl (BP), and E-stilbenyl (ESB) to the bisfluorene core. The researchers spin-coated the dendrimer film on a two-dimensional corrugated fused silica substrate and prepared an optical pump distributed feedback laser that operates in the blue spectrum region. Additionally, they spin-coated a dendritic film on a two-dimensional corrugated molten silicon dioxide substrate to create an optical pump distributed feedback laser with a threshold of 4.5 $\mu J \cdot cm^{-2}$ in the blue spectrum region.

Lai et al. [49,50] reported materials with high solid-state quantum efficiency, an attractive feature for OLED and laser applications. Their research demonstrated that the length of the long fluorene chain is not a necessary condition for effective solid-state luminescence. They extended the third-generation T6-truxene by adding six trees instead of three to the truxene core as the gain medium. Consequently, they constructed the DFB laser and achieved an extremely low excitation threshold of 0.4 nJ/pulse, 1.3 $\mu J \cdot cm^{-2}$.

3.2.4. Conjugated Polymers

Conjugated polymers are among the most significant organic semiconductor materials, known for their high optoelectronic properties even in the solid-state form [51–53]. As a typical four-energy system, conjugated polymers offer several advantages, including easier population inversion, wider absorption spectra, and lower excitation thresholds. Altering the side chain structure of the molecule allows for changing the emission peak position. Consequently, many semiconductor lasers use these polymers as the gain medium. π-conjugated polymers are created from a variety of monomers and can form highly defined and sequentially regulated chains. They may take various forms, ranging from amorphous crystals with excellent optical properties to highly oriented crystals that exhibit better charge transport properties when polarized along the chain axis. Mono-domain polymer chain alignment, due to stronger pump radiation absorption, increases the gain coefficients by approximately 1.9 times compared to spin-coated samples, leading to increased optical confinement and more efficient emission. The spectral position of this peak reveals a

strong correlation with the thickness of the PI alignment layer (15–50 nm) [53]. Therefore, the exploration and application of different π-conjugated polymers play a crucial role in reducing the excitation threshold of OSSLs [54,55].

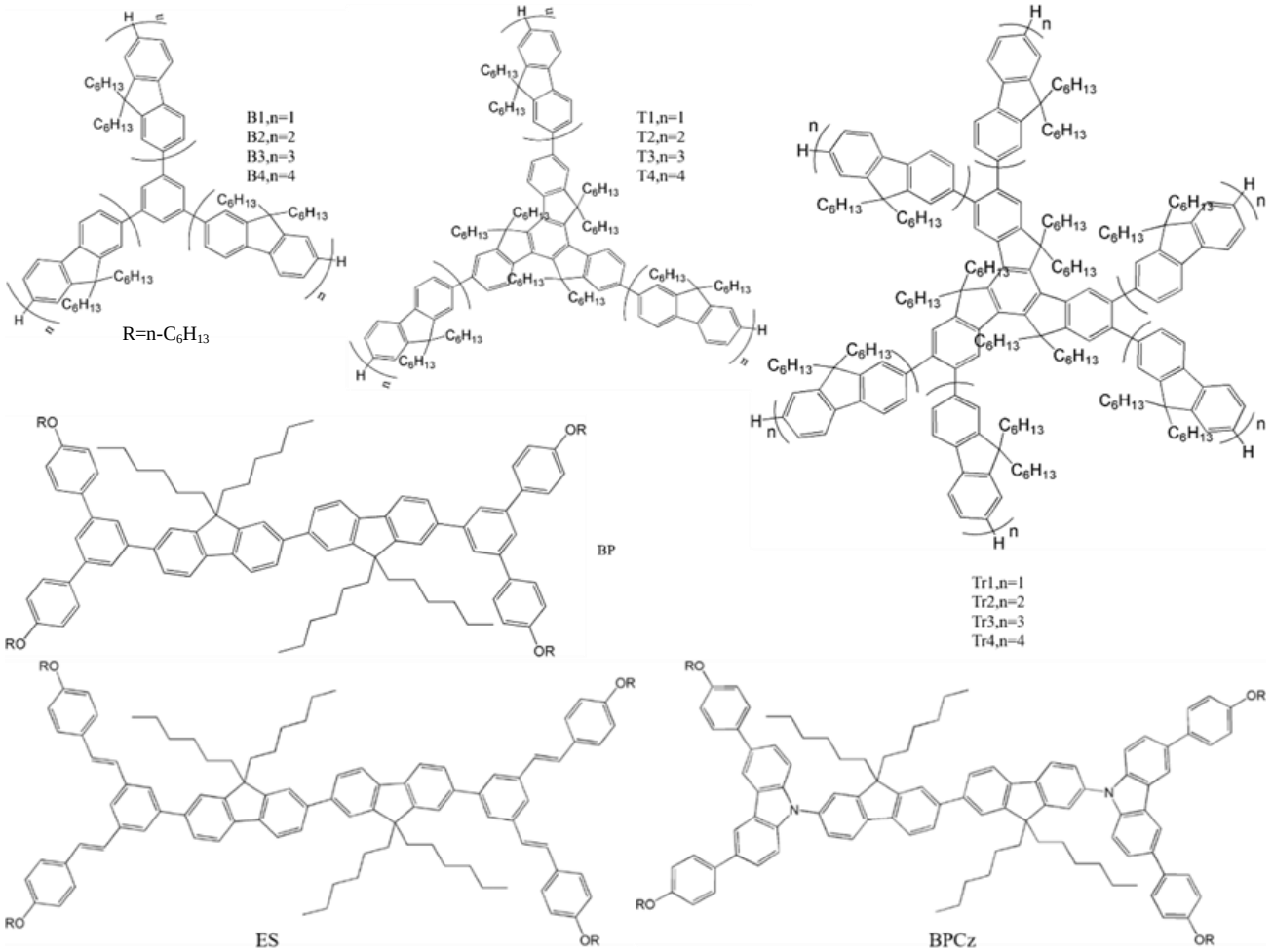


Figure 8. Molecular structures of several dendritic starburst molecules, B1-B4, T1-T4, Tr1-Tr4, BP, BPCz, and ES.

Poly(9,9-dioctylfluorene) (PFO) is a widely used polymer in organic lasers. In polymers with the β-phase morphology, single-oriented molecular chains have extended π-conjugation without π-π accumulation (Figure 9), making it easier to obtain a lower excitation threshold. By using matrix-assisted pulsed laser evaporation (RIR-MAPLE), β-PFO (~6%) pinhole-free films are deposited, resulting in increased carrier mobility [56]. Current investigations on the deviation of the refractive index of amorphous and β-phase polymeric fluorene show it is feasible to construct attractive device geometry with mixed morphology. Compared with the amorphous morphology, the β-phase PFO shows another 430 nm lower energy absorption acromion, resulting in a 1%–2% increase in the refractive index. The β-phase-based PFO DFB laser achieved via spin coating showed a redshift that was a couple of nanometers juxtaposed to the output of the amorphous polymer integrated laser with an identical structure [53]. Alexander et al. [57] reported a crosslinking polyfluorene with vinyl-ether-functionalized aliphatic side-chains (VE-PFO). They prepared an optically pumped DFB laser fabricated from surface-relief gratings in β-phase together with amorphous polyfluorene. By backfilling one form of the grating with the other, it is proven that the threshold (<1 $\mu J \cdot cm^{-2}$) of the device at two wavelengths is at a minimum, ten times below the earlier data.

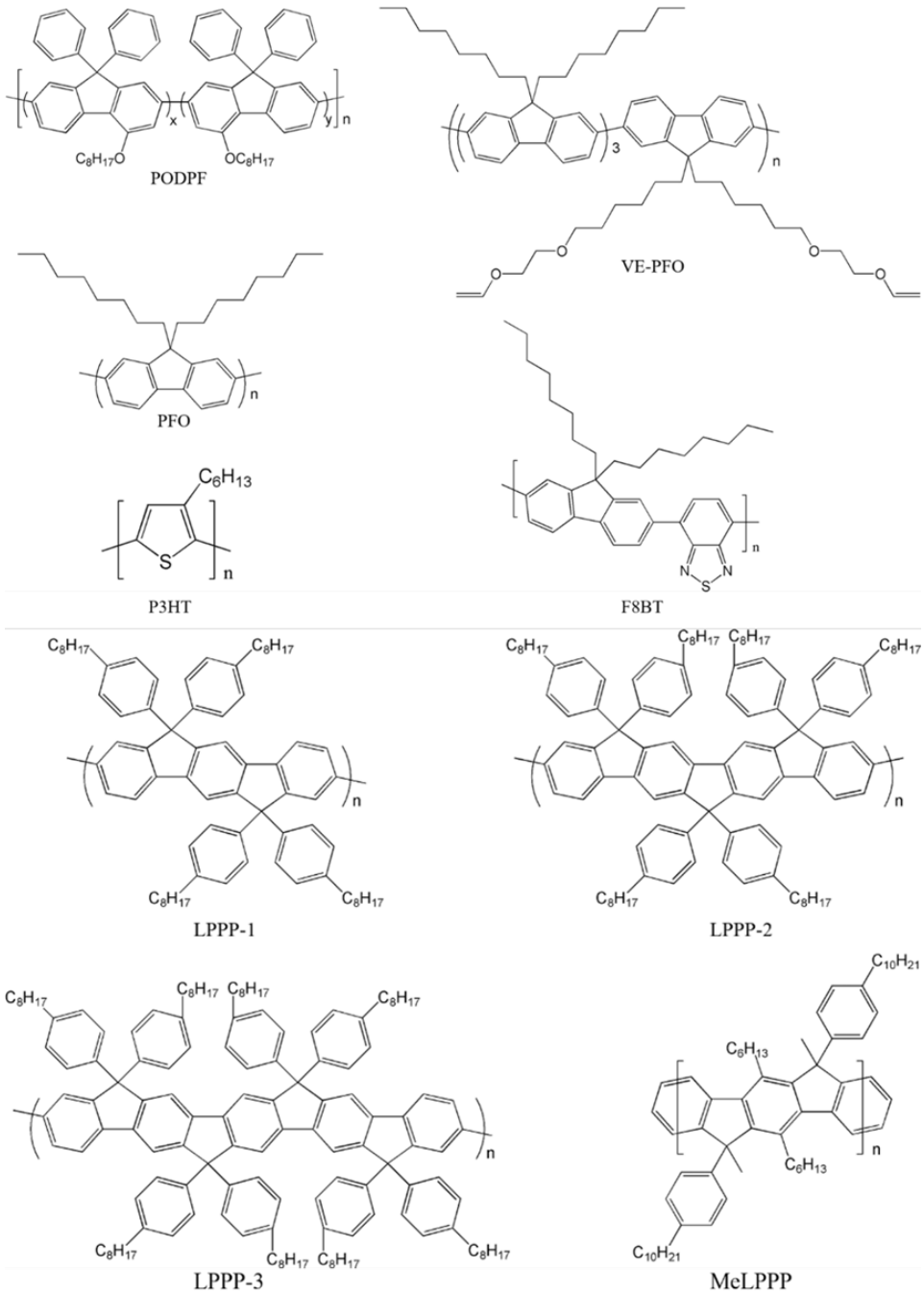


Figure 9. Molecular structures of PODPF, PFO, VE-PFO, P3HT, F8BT, LPPP-1, LPPP-2, LPPP-3, MeLPPP.

Ladder-type poly(p-phenylene)s (LPPP), a relatively famous polymer, is widely used in organic luminescent materials due to its high quantum yield and strong stimulated emission under optical pumping. However, limited by the conventional preparation method, poor oxidative stabilities, and low carrier mobilities caused by incidents, such as interchain-aggregation-induced energy transfer and fluorenone defects, make it difficult for these materials to be used as the gain medium of organic semiconductor lasers. To address this, researchers prepared LPPP designed with a fused conjugate skeleton structure by UV embossing process to improve carrier mobility, reduce the excitation threshold, and apply it to lasers with low thresholds. Kallinger et al. [58] constructed an organic laser with a DFB structure using MeLPPP as the gain medium, achieving a 4.8 $\mu J \cdot cm^{-2}$ excitation threshold. Their deposition was made on a flexible guest, making the device more flexible.

Poly(dioctylfluorene-co-benzothiadiazole) (F8BT) is an extensively employed conjugated polymer in OLEDs today. With a 28 $\mu J \cdot cm^{-2}$ ASE threshold and a yellow-green excitation emission spectrum, it is a potential gain medium for low-threshold semiconductor devices. Xia et al. [59] used a 9:1 fluorene (F8) to benzothiazole (BT) ratio, which differed from the initial 1:1 ratio, greatly increasing the gain of the medium and lowering its ASE threshold to 2 $\mu J \cdot cm^{-2}$. The improvement is attributable to chain separation enhanced because of the octyl side chain, which effectively prevents the destruction of exciton activities and thus significantly reduces the excitation threshold. Additionally, Xia et al. [60] reduced the excitation threshold through a host-guest system of two polymers. They reported the optical gain behavior of poly(dioctylfluorene-co-benzothiadiazole) (F8BT) and regional molecular polymer (3-hexylthiophene) (RR-P3HT) binary blending films. Effective optical gains were noticed in the 10–20 wt. % RR-P3HT composition category, with a pump pulse threshold of merely 8 nJ (26 $\mu J \cdot cm^{-2}$, 2.17 $kW \cdot cm^{-2}$) for a distributed feedback laser with a one-dimensional grating, which is less than alternative polymer-based organic semiconductor materials in this spectral region.

3.3. Other New Materials

Currently, many scholars are focusing their attention on organic materials that have emerged in recent years to improve the modal gain, reduce the excitation threshold, and make low-threshold organic semiconductor lasers a reality [61]. Some of these materials include organic-inorganic hybrid halogen perovskite, known for its high energy conversion efficiency; highly self-arranged liquid crystal materials that can form an optical gap suitable for lasers; green light protein fluorescent protein, commonly used as an imaging tracking material in photonic biology; and deoxyribonucleic acid (DNA) biopolymers doped with fluorophiles.

Perovskites exhibit properties comparable to those of industrial standard silicon for long-distance charge transfer and efficient charge collection. While not technically organic materials, they share several characteristics with organic molecules, classifying them as organic optoelectronic materials for research purposes. Perovskite lasers have [61] high band gap tunability, covering a range from near-infrared to ultraviolet light. They also offer the potential for polarization, exciton, and free carrier excitation, and could potentially be used to create electrically pumped semiconductor lasers [62,63]. Xing et al. [64] reported a low ASE threshold of 12 ± 2 $\mu J \cdot cm^{-2}$ and a carrier density of 1.7×1018 cm^{-3}, which is comparable to the latest solution-treated gain medium. Stranks et al. [63] reduced the threshold flux of ASE by two orders of magnitude in the perovskite film by placing $CH_3NH_3PbI_3$ perovskite film in a cavity made up of a thin-film cholesteric liquid crystal (CLC) reflector and a gold back reflector [64].

Fluorescent proteins represent a range of bioluminescent groups dating back to 1962. Gather et al. [5] demonstrated that fluorescent proteins(4,5) in cells can serve as feasible optical amplification media. They were the first to report a working GFP biological cell laser and demonstrated an in vitro protein laser using a recombinant GFP solution. Additionally, they introduced a laser derived from a single living cell expressing GFP. By using an optical pump of a nanosecond pulse, they produced directional, bright, narrow-band laser emission in a high-Q microcavity with unique longitudinal and transverse modes. The reported working laser threshold was approximately 1 nJ/pulse.

Hung [65] conducted a comparative study of the ASE properties of two dye-doped DNA biopolymers. They achieved efficient energy transfer, resulting in a lower excitation threshold for DNA biopolymers by using suitable surfactants in a system consisting of two surfactant-modified DNA and a doped optical film, where an organic dye Rhodamine 6G (Rh6G) served as the dopant. Incorporating DNA fluorescence enhancement could further promote the application of biopolymers as effective media for lasers and OSSLs. (See Table 2).

Table 2. Transition mechanisms in an organic laser gain medium.

Materials	Threshold (μJ/cm^2)	Reference	Advantages	Disadvantages
PMMA	50	[26]	easy operation	low performance
DNA	3	[27]	Strong inhibition	not easy operate
PM567	1.35	[28]	Strong inhibition	dopant dyes
cis-DCSQ1	10	[29]	good stability	discrete
p-MSB and o-MSB	14	[37]	good continuity	not easy operate
linear oligomer fluorene of hexyl chains	0.4	[41]	good stability	reasonable handling
liquid 9-(2-ethylhexyl)carbazole	2	[42]	good stability	dopant dyes
spiro-SBCz	0.197	[43]	good stability	not easy operate
bisfluorene-cored dendrimers in solids	4.5	[48]	Good self-performance	discrete
T6-truxene	1.3	[49,50]	good continuity	not easy operate
VE-PFO	1	[57]	Strong inhibition	discrete
LPPP	4.8	[58]	More flexible	low performance
F8BT	26	[60]	easy operation	dopant dyes
Perovskite	12	[64]	good stability	discrete

4. Measures of Threshold Reduction of Optically Pumped Organic Laser in Terms of Structures

An effective approach to achieving low-threshold organic semiconductor lasers involves improving the resonator's structure. This enhancement enables multiple reflections of light within the gain medium while reducing optical loss at the reflector interface [66,67]. This aspect is crucial in the fabrication of organic lasers. Additionally, a high-Q optical microcavity proves to be an efficient property that can be harnessed to lower the excitation threshold. In micro-nanoscale semiconductor lasers, optical feedback structures are constructed using the gain medium itself, which represents a prominent research area in organic optical microcavities.

Currently, commonly employed optical feedback structures include the plane cavity, distributed feedback structure, organic crystal cavity [68,69], WGM resonator, and organic nanowire structure, among others. Most researchers begin their investigations with these structures, aiming to innovate and explore higher-quality optical microcavities at the micro-nano scale level. The ultimate goal is to construct organic laser devices with lower thresholds.

4.1. Plane Cavity

The original organic lasers were based on a macroscopic structure consisting of a pair of mirrors and liquid or solid organic dyes, which typically resulted in a large energy output. However, their lack of convenience failed to meet the requirements for organic lasers. The linear Fabry–Perot microcavity was the first optical microcavity used in solid-state organic semiconductor lasers. In this structure, the reflector is usually achieved through the interface of two materials with a high refractive index. For instance, Kozlov et al. [15] demonstrated a planar cavity organic semiconductor laser constructed with an Alq3:DCM host and a visitor system as the gain medium. The laser action of Alq3/DCM between SiO_2 (n = 1.4) and air (n = 1) cladding and the laser action of Alq3/DCM film sandwiched between two 125 nm Alq3 cladding layers used to construct a planar cavity structure were confirmed to achieve a lower excitation threshold of about 1 μJ·cm^{-2}. To enhance the reflector's limiting effect and increase reflectivity, a reflector is often constructed with a metal layer deposited via thermal evaporation or a distributed Bragg mirror (DBR) reflector (Figure 10a). The DBR reflector is typically formed by alternating oxides with different refractive indices. The DBR structure can increase the microcavity's reflectivity to higher than 99%, significantly boosting the Q value and effectively reducing the excitation threshold. Gather et al. [70] constructed a vertical cavity surface emitting laser (VCSEL)

with the gain material composed of a thin sheet of enhanced green fluorescent protein (eGFP) inserted between two highly reflective DBRs, with a low excitation threshold of <100 pJ. Oxide or metal reflectors usually require electron beam evaporation or sputtering for deposition, which may cause damage to the organic film serving as the gain medium. For this reason, Canazzaet et al. [71] demonstrated a microcavity structure of DBR reflectors constructed with polymers. The DBR reflective films were prepared via spin-coating cellulose acetate and polyvinylcarbazole orthogonal solutions. The gain material films were achieved by spin-coating the highly fluorescent conjugated polymer F8BT as the gain medium. Using pulsed light pumping, a low excitation threshold < 20 $\mu J \cdot cm^{-2}$ was obtained for laser emission in the polymer DBR microcavity. (See Figures 10 and 11).

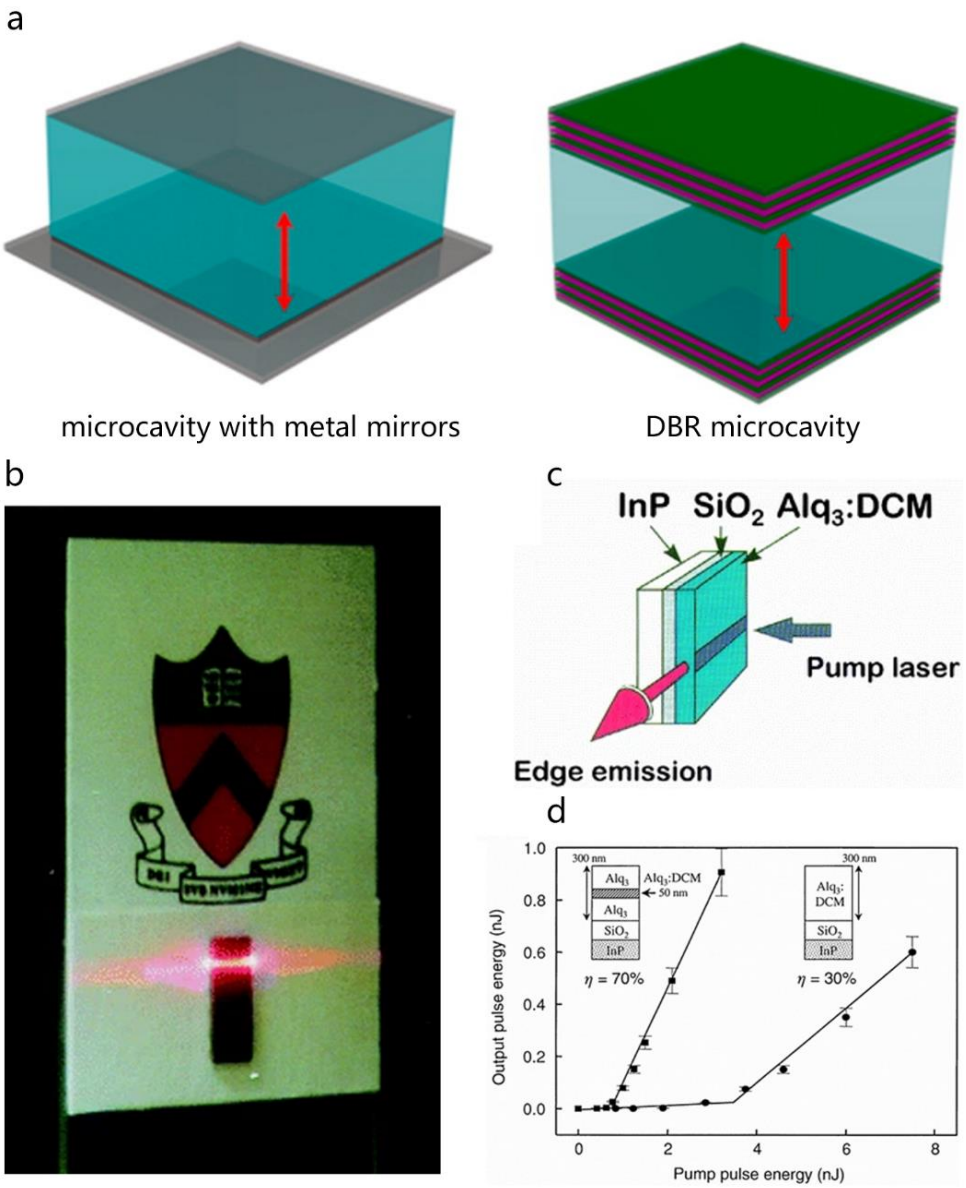


Figure 10. (**a**) Schematic of microcavity with metal mirrors and the structural representation of DBR microcavity [2]. Copyright 2016 Chemical Reviews (**b**) Picture of the Alq3/DCM slab-waveguide red laser. (**c**) Schematic of the laser structure and experimental setup. (**d**) The output energy as a function of the input pump energy around the threshold for 1-mm-longslab-waveguide (**right** inset) and double-heterostructure (**left** inset) laser devices whose structures are exhibited. (**b**–**d**) [15] Copyright 1997 Nature.

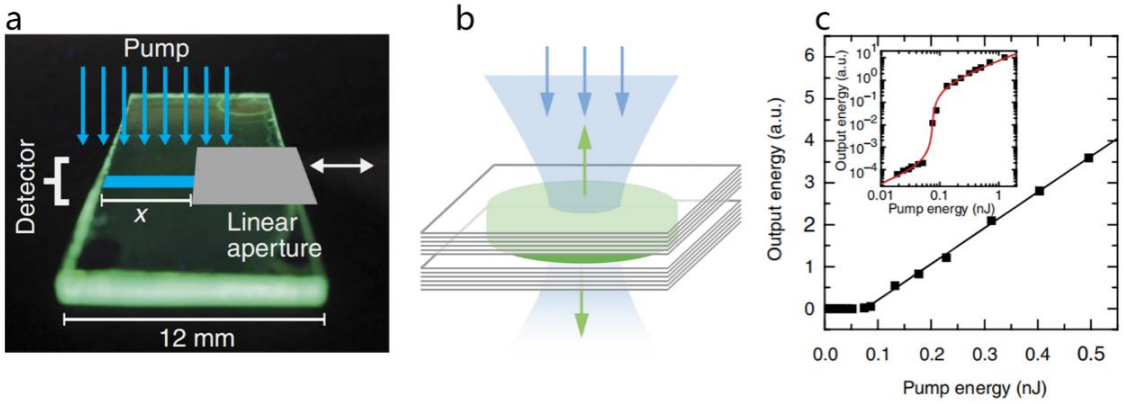


Figure 11. (**a**) A photograph of eGFP film on a glass guest with the ASE measurement depicted. (**b**) VCSEL schematic consisting of a thin layer of eGFP as gain medium inserted between two ultra-reflective Bragg mirrors. (**c**) Dependence of the output of eGFP VSCEL on the pump pulse energy (filled squares). Inset: Fit model of the same data employing the rate equation model, illustrated on log-log scale. (**a**–**c**) [70] Copyright 2014 Nature communications.

4.2. Distributed Feedback Structure

The planar microcavity structure is simple and easy to prepare, but it lacks the transverse limiting effect and easily generates high scattering loss at the interface. The device as a whole has low reflectivity and high requirements for interface quality. On the other hand, the distributed feedback (DFB) structure can realize the long interference of light with a specific wavelength by relying on periodic diffraction gratings [23], which provide higher efficiency feedback for the lasers and make organic lasers with low thresholds possible.

To form the DFB structure, a gain medium organic material film is usually prepared on a substrate with a grating structure surface to create a wavy structure. This structure establishes a waveguide mode of reflection propagation without the need to form an end face. Many different diffraction structures have been explored, including one-dimensional (1D) DFB structures, two-dimensional (2D), and three-dimensional (3D) photonic crystal structures (Figure 12).

In the DFB structure, the light waves traveling within the waveguide of the organic film experience scattering by cyclical ripples. Constructive interference occurs at the wavelengths of the light scattered by different ripples. Bragg scattered waves with different wavelengths are formed by scattering and coherence, spreading in different directions [72]. For a specific grating period, only the light with a specific wavelength can generate constructive interference and feedback in the opposite direction of the incident wave, thus achieving laser emission. The bandwidth of the feedback light wave (the band gap width near the central Bragg wavelength) is correlated with the depth of the ripple. The central Bragg wavelength can be described as follows:

$$m\lambda_{Bragg} = 2n_{eff}\Lambda \quad (1)$$

Among them, m represents the series of diffraction (an integer), λ_{Bragg} denotes the laser emission wavelength, n_{eff} indicates refractive index of the waveguide, Λ signifies the grating structure cycle. The wavelength of a reflected light for a first-order diffraction is twice $n_{eff}\Lambda$. Therefore, a secondary structure can generate a laser surface emission output coupling through the first-order diffraction, and, at the same time, provide in-plane feedback through the second-order diffraction prior to achieving surface emission. Although the threshold of second-order diffraction grating is higher than that of first-order grating, it is the more advantageous option for a laser output [73].

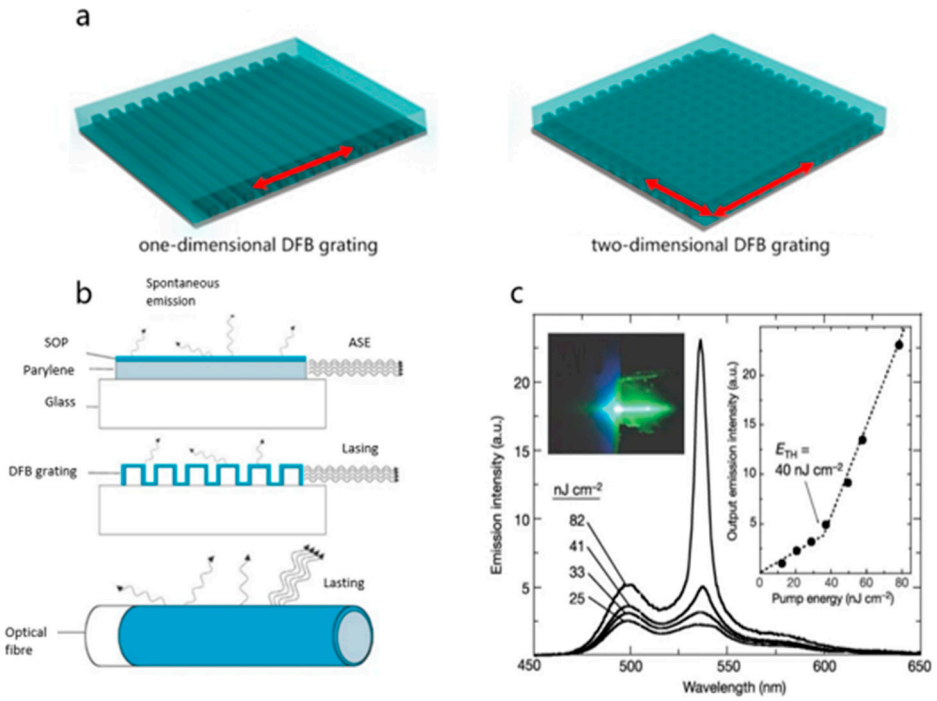


Figure 12. (**a**) Schematic of microcavity with one-dimensional DFB grating and two-dimensional DFB grating [2]. Copyright 2016 Chemical Reviews (**b**) Schematic of test structures displaying lasing chemosensory responses. (**c**) Polymer1′s spontaneous and stimulated emission above polydimethylsiloxane DFB structures. Stimulated emission threshold (ETH) of 40 nJ·cm^{-2} was illustrated by the emission spectra of polymer 1 structures and previous figure with pump energies changing, which is low-valued. Left inset, a pulsed light of λ = 337 nm is pumped to polymer 1 film (**right** part of the image), leading to an orientational radiation output (**left**) exceeding the threshold pump energy. Right inset, the diagram of input power and output intensity at λ = 535 nm peak. (**b**,**c**) [74] Copyright 2005 Nature.

The high reflectivity of the DFB structure makes it easy for the laser to achieve a very low laser threshold. Rose et al. obtained a threshold energy of ETH = 40 nJ·cm^{-2} in the organic polymer film of the DFB structure and achieved an ultra-low side-pumping threshold density of 200 nJ·cm^{-2}, a level that is difficult to reach with other forms of micro-cavity structures.

Karnutsch et al. [74,75] reported a distributed feedback laser with an improved resonator structure. By combining the superiorities of first-order and second-order DFB gratings, they constructed a resonator structure surrounded by a first-order scattering region of second-order gratings, providing high-efficiency vertical output coupling. This method generated strong feedback. The gain medium of the laser used was a conjugated polymer poly [9,9-dioctylfluorene-co-9,9-di(4-methoxy-phenyl)fluorene] thin film, which realized the threshold as low as 45 pJ/pulse (about 36 nJ·cm^{-2}).

Furthermore, Karnutsch et al. [76] constructed a polymer DFB laser that obtained an extremely low excitation threshold and was made of a polyfluorene derivative, which includes statistical binaphthyl units (BN-PFO). The threshold energy of the second-order DFB structure was found to be 280 pJ/pulse. Moreover, it could be further decreased to 160 pJ/pulse by using the first-order feedback in the electron beam photolytic structure with a 140 nm cycle.

In addition to the 1D DFB laser described above, the 2D DFB structure has also attracted the attention of many scholars. This complex diffraction grating can limit the propagation of light waves in both directions in the waveguide and introduces a 2D DFB structure in the plane of the organic semiconductor film, which is beneficial to increase reflectivity and theoretically reduce the excitation threshold. At present, lasers have been

generated in 2D DFB structures, such as squares [77–79], hexagons [80,81], and concentric circles [82]. Heliotis et al. [79] constructed a resonator structure based on PFO that can provide unidirectional and 2D distributed feedback. This 2D DFB laser works in the blue spectrum and has a slope efficiency of up to 7.8% and an oscillation threshold energy as low as 0.8 nJ/pulse. Turnbull et al. [83] constructed an all-solid surface emitting 2D DFB laser using a microchip laser as the optical pump source. The laser's gain medium was the conjugated polymer poly(2-methoxy-5-(2(′)-ethylhexyloxy)-1,4-phenylene vinylene), which reached the excitation threshold of 4 nJ. In fact, the advantages of the DFB structure are not only reflected in the threshold reduction but also in its ability to select light in the resonant spectrum beyond any other type of microcavity structure. Additionally, the second-order grating, specifically, can realize surface emission, which expands the application range of the organic laser (Figure 13). It also simplifies the use of light sources with poor collimation or decent collimation in optical pumping, which proposes a pathway for the indirect electric pumping of organic laser devices. Under short-pulse photoexcitation, the mixed-order circular DFB grating structure presents the lowest lasing threshold of 0.015 μJ·cm^{-2} among 2D grating structures in any BSBCz-based laser device. Through simulation and experimentation, it provides guidelines for the design and optimization of 2D gratings, making it possible to fabricate CW-operating OSLDs [84].

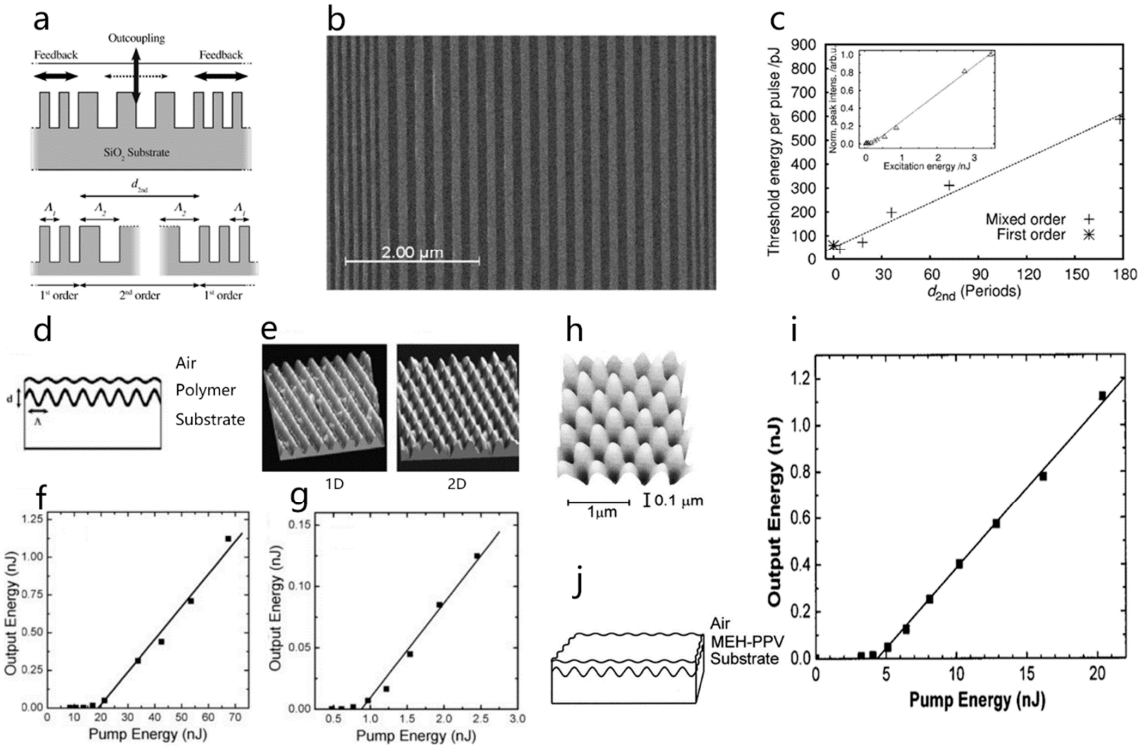


Figure 13. (**a**) Height-outline of the mixed-order gratings, comprising two first-order sections, which produce feedback and a second-order region for vertical outcoupling. (**b**) Scanning electron microscope (SEM) image of a mixed-order grating which includes 18 periods in the second-order region. (**c**) Threshold energy of mixed-order grating lasers for differing d2nd period numbers in the second-order region. Inset: Input–output features of a mixed-order laser with d2nd equaling 36 periods. The laser threshold energy is about 200 pJ. (**d**) Schematic of the DFB laser structures. (**e**) Atomic force microscopy (AFM) images of the 1D and 2D DFB grating silica guests. (**f**) Dependence of the output energy from the 1D PFO DFB laser on the pump energy. (**g**) Plot of output energy from the 2D PFO DFB laser versus the pump energy. (**h**) AFM image of the surface of the silica guest. (**i**) Output energy from polymer laser represented in the graph as a function of pump energy. (**j**).Waveguide structure of DFB laser. (**a**–**c**) [75] Copyright 2007 Applied Physics Letters. (**d**–**g**) [79] Copyright 2004 Advanced Functional Materials (**h**,**j**) [83] Copyright 2003 Applied Physics Letters.

4.3. Whispering Gallery Mode Resonators

Organic semiconductor materials possess relatively good characteristics for solution treatment and can form complex structures that are not achievable with inorganic materials. For instance, microfluidic operations or other solution treatment processes can create whispering gallery mode (WGM) resonators with low roughness and high Q values, enabling the production of organic laser devices at a lower cost. In a WGM resonator (Figure 14), light waves are reflected multiple times on the ring or sphere of organic gain mediums, which have a refractive index higher than that of air, forming a circular standing wave. When this wavelength aligns with the gain spectrum of the gain medium, the light gets amplified within the structure significantly [68], reducing the excitation threshold. A [85] WGM resonator typically attains a high Q value, which is mainly associated with the surface roughness of the cavity interface. The microfluidics process allows the preparation of disc or spherical WGM microcavities with an exceptionally smooth surface due to surface tension, resulting in a flat gas–liquid interface at the atomic level. (See Figure 14).

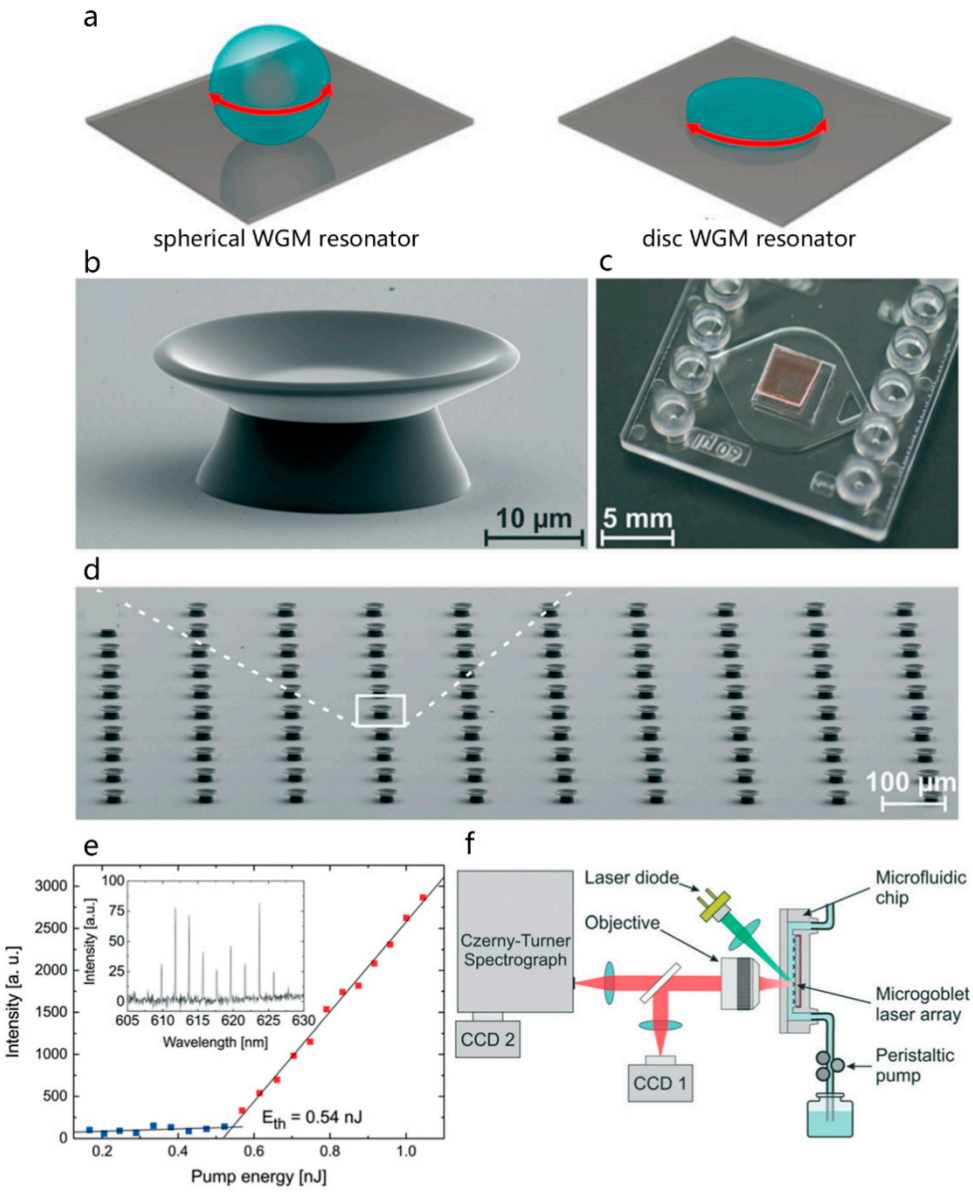


Figure 14. (**a**) Schematic of spherical WGM resonator and disc WGM resonator [2]. Copyright 2016 Chemical Reviews (**b**) SEM image of a single PMMA microgoblet laser based on a polymer pedestal

developed using lift-off resist. (**c**) Photograph of a sensing chip: 100 microgoblet lasers array fabricated as a microfluidic integrated chip. Transparency of the chip permits optical addressing of individual microgoblets via the lid in free-space optics. (**d**) Parallel solution-based processed array of 100 microgoblet lasers. (**e**) Input–output characteristics of a WGM microgoblet laser emitting at a wavelength of 623.7 nm. (**f**) Illustration of the photonic LoC system: the all-polymer chip consists of an array of microgoblet lasers integrated into a microfluidic channel. (**b**–**f**) [86] Copyright 2015, Lab on a chip.

Wienhold et al. [86] produced a PMMA whisper gallery mode microgoblet resonator doped with organic dye pyrromethene 597 on a microfluidic chip using rotation coating, mask optical lithography (Figure 15), wet chemical etching, and thermal reflux. The device exhibited a laser threshold of less than 0.6 nJ/pulse, enabling efficient pumping through compact, low-cost green laser diodes and free-space optical devices. Grossmann [69] reported the fabrication of conical rhodamine 6G-doped high-Q conic polymer microcavities on a silicon guest. In the quasi-static pumping state with a laser wavelength of about 600 nm, a low threshold pumping energy of 3 nJ was achieved by free-space excitation. The WGM resonator structure was first realized specifically in the shape of micro-rings. For organic polymer materials, the optical fiber can be directly immersed in the organic solvent to form a circular micro-cavity [66], where the light bounces off the interface between the polymer and the encompassing medium, forming a waveguide. Since optical fibers are typically a few millimeters in diameter and light waves travel long distances around the fiber, the feedback mode is usually a mixture of a whispering gallery mode and a waveguide mode. Rotschild [67] rotated the first terylene in the PMMA guest on a silicon dioxide microplate and evaporated the mixture of 4-(dicyanomethylene)-2-t-butyl-6-(1,1,7,7-tetramethyljulolidyl-9-enyl)-4H-pyran (Alq3: DCJTB) onto the resonator, where the incoherent light was converted into coherent light with an elevated quantum efficiency [87]. The effective energy transfer from Alq3 to DCJTB and tritoluene materialized with a 5 $\mu J \cdot cm^{-2}$ excitation threshold under the action of a UV pump.

4.4. Organic Crystal Cavity

The organic crystal surface can form effective reflections, providing high-quality light feedback. Therefore, organic crystals can serve not only as gain media but also as optical resonators. In organic crystals, one method to construct the optical feedback structure is by using the faceted end crystal as the Fresnel reflection. The group refractive index of organic crystals can be as high as 3.5, and the cavity length can be on the order of 100 μm. The Fresnel reflection generated at the crystal–air interface is only about 30%. However, the Q factor in a single crystal Fabry–Perot cavity is reported to be more than 1000 [88,89]. This is because the crystal cavity is longer than the traditional cavity, several times the length of $\lambda/2$, allowing it to output a laser with a wavelength of λ [90]. Apart from the geometry of the Fabry–Perot resonator, the organic crystal cavities have square or hexagonal structures similar to the WGM resonator, providing stronger internal reflection and better light restriction. In recent years, many examples of these structures based on different small molecular materials have been reported [91,92], the excitation threshold of the organic crystal cavity is still currently limited to a relatively high level. (See Figure 16).

4.5. Structure of Organic Nanowires

Semiconductor nanowires offer a promising platform for the future development of electrically pumped organic lasers [89], thanks to their defect-free structure and exceptional electrical transmission characteristics [90]. Fibers and nanowires can be employed to create Fabry–Perot resonators with microscopic dimensions [91], incorporating gain materials within the fibers [92]. Camposeo et al. [93] obtained submicron-diameter fibers by dissolving small fluorescent molecules in a PMMA solution and subsequently electrospinning them. The mixture of small fluorescent molecules in the PMMA solution was electrospun to achieve submicron diameters ranging from 100 to 600 nm, capable of emitting light at a

threshold of 60 μJ·cm2. In this setup, the fiber serves as an optical waveguide, with its end face acting as a reflector to provide light feedback.

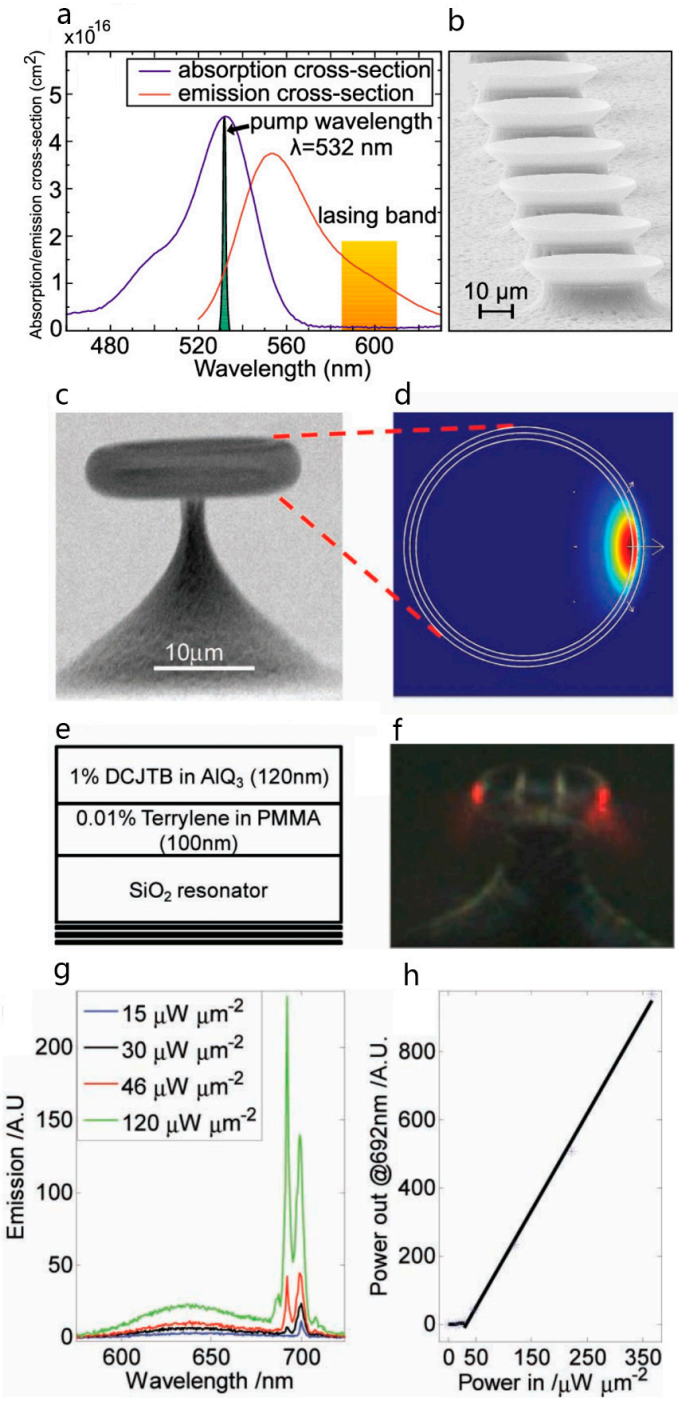


Figure 15. (**a**) Absorption and stimulated emission cross-section of rhodamine 6G molecules planted in PMMA and pump wavelength and lasing band of the microcavity lasers. (**b**) SEM micrograph of an array of conical polymeric microcavities with a peak diameter of 40 μm. (**a**,**b**) [69] Copyright 2010 Applied Physics Letters. (**c**) SEM image of A typical micro-ring resonator. (**d**) Numerical simulation of the lasing mode with polarization designated by the arrows. (**e**) Schematic of the gain materials fabricated on the resonator. (**f**) A typical example of lasing (**g**) Progression of the emission spectrum at different pump intensities. (**h**) Lasing power at λ = 692 nm as a function of pump power showing lasing power threshold at 30 μW·μm^{-2}. (**c**–**h**) [67] Copyright 2011 Advanced Materials.

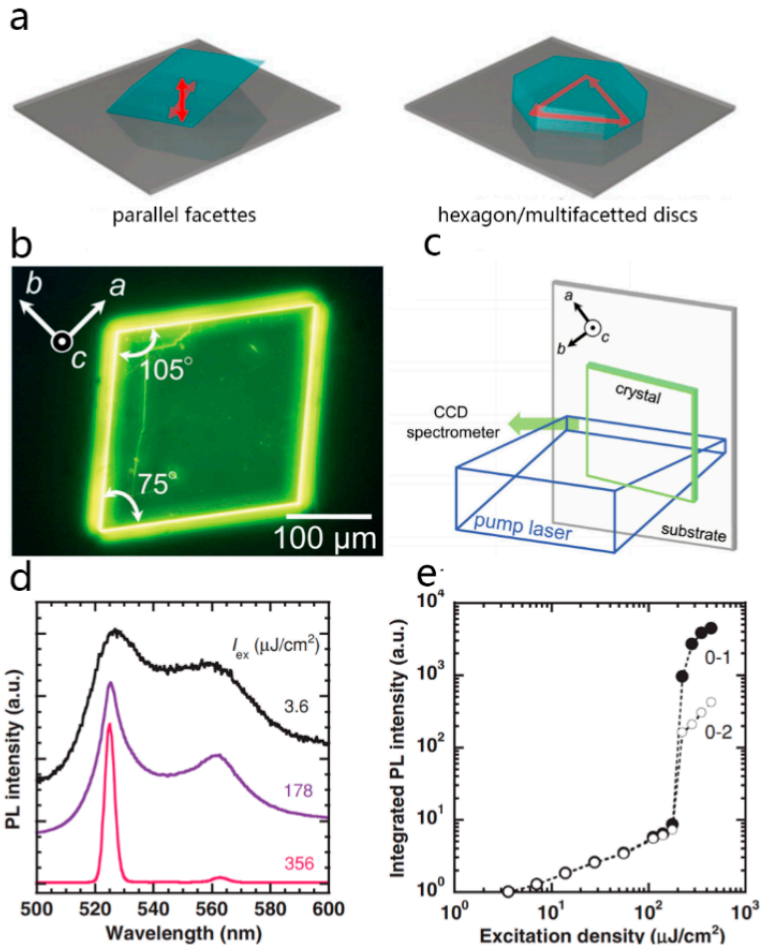


Figure 16. (**a**) Schematic of microcavity with parallel facets and hexagon/multifaceted discs [18]. Copyright 2016, Chemical Reviews (**b**) Fluorescence image of single-crystal BP2T-OMe excited at 365 nm. (**c**) Illustration of the optical measurement setup where a stripe-shaped excitation beam was struck perpendicularly across the parallel {110} facets of BP2T-OMe crystal. The light emitted from the crystal edges was detected along the stripe path. (**d**) Correlation between excitation density and PL spectra excited at λ_{ex} = 397 nm. (**e**) Integrated intensities of the 0–1 and 0–2 bands dependence on the excitation density. (**b**–**e**) [88] Copyright 2012, Advanced Materials.

Benedetto [94] used conjugated polymers to create electrospun fibers, creating a nonwoven pile entirely composed of gain materials. These electrospun composite polymer fibers were imprinted with periodic gratings through room-temperature nano-imprint lithography, significantly enhancing the waveguide capability along the fiber. While this structure can be utilized in DFB (Distributed Feedback) lasers based on fiber, laser emission has not been demonstrated yet. (See Figure 17).

4.6. Structure of Film

In addition to gaining the material and resonant cavity, the characteristics of the film should also be taken into consideration. By varying the film thickness from 100 to 200 nm, the position of ASE (Amplified Spontaneous Emission) can be tuned between 404 and 407 nm, influenced by the waveguide mode [95]. This demonstrates that changing the thickness can lead to a Stokes shift, causing variations in the laser threshold. Moreover, a lower laser threshold can be achieved after annealing, resulting in a regular crystal orientation distribution.

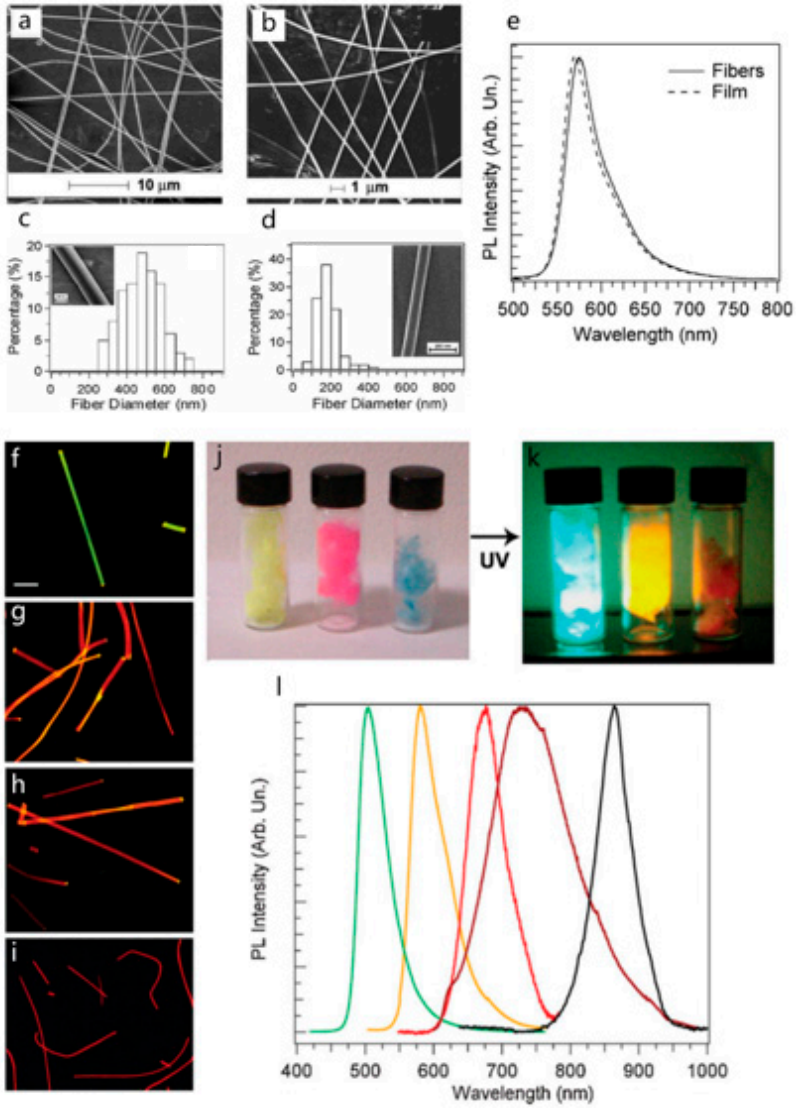


Figure 17. (**a**) SEM micrographs of fiber with an applied voltage of 15 kV. (**b**) SEM micrographs of fiber with a higher applied voltage of 27 kV. (**c**) Diameter distributions of fiber for mats spun with a voltage application of 15 kV. Inset: SEM images of single nanofibers. (**d**) diameter distributions of fiber for mats spun with a 27 kV voltage application. Inset: SEM images of single nanofibers. (**e**) PL spectra of fiber mats (continuous lines) integrating R6G as gain molecule, and PL spectra of the correlating reference films (dashed lines). (**f**–**i**) Fluorescence images of fibers with Coumarin 334 (**f**), R6G (**g**,**h**), and Nile Blue (**i**). Scale bar: 10µm. (**j**,**k**) Pictures of gain nanofibers experiencing white (**j**) and UV (**k**) light. Images from left to right show the fibers of Coumarin 334, R6G, and Nile Blue A Perchlorate. (**l**) Nanofiber PL spectra experiencing excitation with laser light of 3.05 eV. From left to right, spectra from fibers incorporating Coumarin 334, R6G, Nile Blue A Perchlorate, 2-(8-(4-p-Dimetyhlaminophenyl)-2,4-neopentylene-1,3,5,7-octatetraenyl)-3-methylbenzothiazolium Perchlorate, and 5,5′-dichloro-11-diphenylamino-3,3′-diethyl-10,12-ethylenethiatricarbocyanine Perchlorate. (**a**–**i**) [93] Copyright 2009 Small.

5. Measures of Threshold Reduction of Optically Pumped Organic Laser

Although optical-pumped solid-state organic semiconductor lasers were developed as far back as 1996. To date, a complete and effective demonstration of organic semiconductor laser solutions is still lacking. Nevertheless, the advantages of semiconductor organic lasers [8,96,97], which include a wide spectrum range and large area preparation, have driven the studies of numerous researchers. The realization of electric pumping is the key and most difficult step in positioning the organic semiconductor laser as a realistic

device. In electrically pumped organic semiconductor lasers, the concept behind decreasing the excitation threshold is similar to that of optical pumps. It encompasses two aspects: increasing modal gain and reducing modal loss. However, in contrast to the method behind optical pumping, it is very challenging to achieve the threshold condition via electric pumping in organic films. This is primarily because the carrier mobility is low in organic films. Hence, unlike optically pumped organic laser devices, the electric pumping devices need to add a carrier transport layer, an exciton limiting layer, an electrode, and other functional layers, which will significantly increase the mode loss. The losses of electrically pumped organic laser devices can specifically be divided into losses of triplet excitons, dipoles, and electrodes, leading to higher excitation threshold conditions. Thus, manifesting the prevailing difficulties in the research of electrically pumped organic laser devices. In order to achieve the goal of a low excitation threshold, researchers have proposed two different ideas. The first is to solve or reduce the loss of triplet excitons through different material doping systems, and the second is to investigate the structure design to improve the carrier transmission efficiency, reduce the loss of dipoles and electrodes, and construct the resonator with low loss, thereby reducing the excitation threshold and making the electrically pumped laser device a reality.

5.1. Building a New Doping System to Reduce the Influence of Triplet States

Electrically pumped organic laser devices share many similarities with OLEDs in terms of structure and material. However, the rapid development of OLEDs has not guided the progress of organic laser diodes. The most significant breakthrough in the OLED field is the application of the triplet exciton in phosphorescent materials, which greatly improves the luminous efficiency of OLEDs, as seen in Figure 18 [98]. Unfortunately, in organic semiconductor lasers, phosphorescence and triplet exciton are not applicable and are even avoided due to the overlap of the absorption spectrum of the triplet states with the emission spectrum of organic materials [99]. This overlap leads to a parasitic effect of absorption, resulting in a considerable increase in modal loss and threshold. Moreover, triplet excitons accumulate over time, restricting the laser device to only run for a few nanoseconds, significantly hindering the continuous operation of organic lasers.

In the exploration of electrically pumped organic laser diodes, researchers still use similar optically pumped organic lasers with different doping systems, as mentioned above, to achieve Stokes energy transfer and reduce the excitation threshold. This paper will not delve deeper into this excess elaboration. Wallikewitz employed [100] holographic photolithography to produce a DFB resonator using a green-emitting oxetane-functionalized poly(spirobifluorene) named X-LEP as the gain medium, chosen for its optimal optical and electrical characteristics. The electrodes (PEDOT: PSS anode and Ba/Ag cathode) have a photodecoupled refractive index through a low refractive index cladding layer, acting as a charge transport layer, and ultimately limiting the light to the gain medium. The thickness of the cladding is a compromise between optical efficiency (more efficient when thicker) and electrical characteristics (more efficient when thinner). This method realizes a low-threshold optical pumping device and demonstrates its electrical capability, providing an effective concept for the conversion of laser devices from optically pumped to electrically pumped.

Sandanayaka of Kyushu University in Japan reported an electrically pumped organic laser diode that utilizes an excellent performing gain medium, BSBCz, along with an MoO_3 layer for hole injection [101] and BSBCz doped Cs to promote electron injection into the emission layer. The PLQY of BSBCz was close to 100%, with extremely weak triplet exciton generation and negligible triplet exciton absorption, greatly reducing triplet exciton loss. The device also integrated a hybrid order DFB grating to provide sufficient vertically coupled laser radiation. At a current of 600 A/cm2, a clear threshold of the slope efficacy of the laser output was identified, and the FWHM at 480.3 nm was less than 0.2 nm, confirming the successful production of the laser. Although this work has faced some skepticism in the

industry, its material use, structural design, and excellent experimental results represent a major breakthrough in the exploration of electrically pumped laser diodes.

Furthermore, triplet-induced singlet quenching can be overcome by carefully designing organic materials with high PLQYs and ensuring spectral separation of the emission from the excited-state triplet absorption. Alternatively, triplet quenchers like oxygen, cyclooctatetraene, and anthracene derivatives can be used to circumvent triplet accumulation.

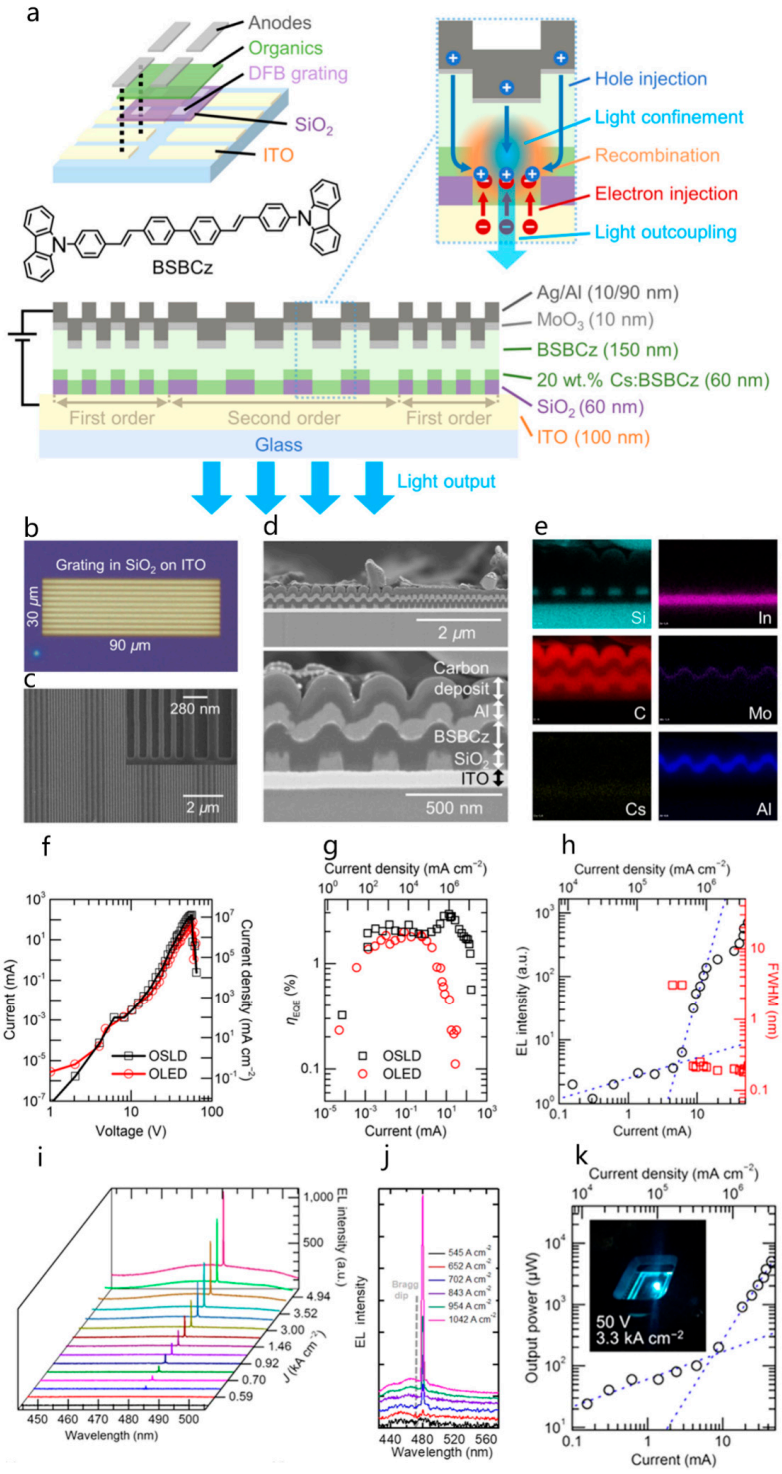


Figure 18. (**a**) Schematic representation of the OSLD. (**b**) Laser microscope image of the DFB grating in SiO_2 on ITO. (**c**) SEM micrographs at 5000× and 200,000× (inset) magnification of a DFB grating.

(**d**) Cross-section SEM representations of the OSLD. (**e**) Cross-section EDX images of the OSLD. (**f**) Current density-voltage (J-V) curves of the OLEDs and OSLDs under pulse operation. (**g**) η_{EQE}-current (η-J) curves of the OLEDs and OSLDs under pulse operation. (**h**) The dependence of output intensity and FWHM on the current and current density. (**i**) Emission spectra of an OSLD gathered in the direction normal to the guest plane for various injected current densities. (**j**) Emission spectra near the lasing threshold. (**k**) A plot relating the output power to the current. A picture of an OSLD experiencing pulse operation of 50 V (insert). (**a**–**k**) [101] Copyright 2019, Japan Society of Applied Physics.

5.2. Improving Carrier Transmission Efficiency and Reducing Losses through Structural Design

5.2.1. Improving Device Carrier Transport Efficiency

In the exploration of electrically pumped organic laser diodes, besides constructing a reasonable material doping system to reduce the impact of triplet states, researchers commonly use innovative device structures. This technique is essential to solve the current challenges faced by electrically pumped devices and achieve a low excitation threshold. Unlike traditional OLED devices, electrically pumped laser devices require higher carrier injection and higher carrier transmission efficiency (Figure 19). Therefore, it is crucial to break the limitations of the original structure and design a new carrier transmission structure. Additionally, to reduce dipole and electrode losses and construct a resonator with low loss and reduced excitation threshold, the structure needs to be innovated and optimized.

The excitation threshold of optically pumped thin film organic semiconductor lasers usually needs to reach a range of $\mu W \cdot cm^{-2}$. For electrically pumped laser devices like the Alq3:DCM system [102] and the DFB laser [103] in the PPV system, a driving current density of 200 $A \cdot cm^{-2}$ is required to avoid additional losses. Achieving such a high current density requires a very high charge density, but excessive charge aggravates the quenching of polarons and tripletons. Polarons have a broad spectral absorption range, and when this range overlaps with the gain medium's emission spectrum, additional losses occur. By optimizing the device structure and improving carrier transport efficiency, the needed polaron density to obtain a given current can be reduced, helping to restrict polaron annihilation. Therefore, optimizing the structure to improve carrier transport efficiency is not only necessary to reach the required energy density but also an effective way to reduce polaron and other losses. Tessler [104] optimized the structure of an LED to be driven by a high current with a short pulse, achieving a high current density in the $kA \cdot cm^{-2}$ range and greater carrier transmission efficiency. However, due to the extra loss in the electric pumping mode, laser emission cannot be realized at such a high charge density. Using an organic/inorganic hybrid design is an effective strategy to improve carrier mobility and reduce charge density in organic materials. Song [105] constructed a DFB grating structure containing an organic PFO emission layer between a relatively thick inorganic hole transport (MoO_3) layer and an electronic transport (ZnO) layer, combining the high carrier transmission rate of inorganic materials with the high luminescence efficiency of organic materials. This design successfully enhanced carrier mobility and decoupled the electrode from the emission organic layer, supporting waveguide TE2 modes firmly restricted to polyfluorene gain materials, thus creating a relatively efficient optically pumped laser. Although spontaneous electroluminescence was observed under electrical pumping, no electrically pumped laser was achieved [106].

5.2.2. Reducing Electrode Loss

Due to the requirement for carrier injection, the primary distinction between electrically pumped organic laser devices and optically pumped ones lies in the employed electrode. Currently, the cathode used in OLED devices needs to be made of metal materials, but the reflectivity of metal films is low (Ag has a reflectivity as high as 95%, while common Al is below 92%). These electrodes have a wide absorption range and a large absorption coefficient, which can cause a significant loss of light. Therefore, inhibiting the loss of metal electrodes is necessary to construct high-quality optical microcavities and reduce

the excitation threshold. One relatively simple treatment method is to use a transparent conductive oxide to replace the metal as the electrode of an organic laser device [107]. However, in practice, the transparent conductive oxide electrode is also highly absorbent and is challenging to effectively reduce the excitation threshold [108].

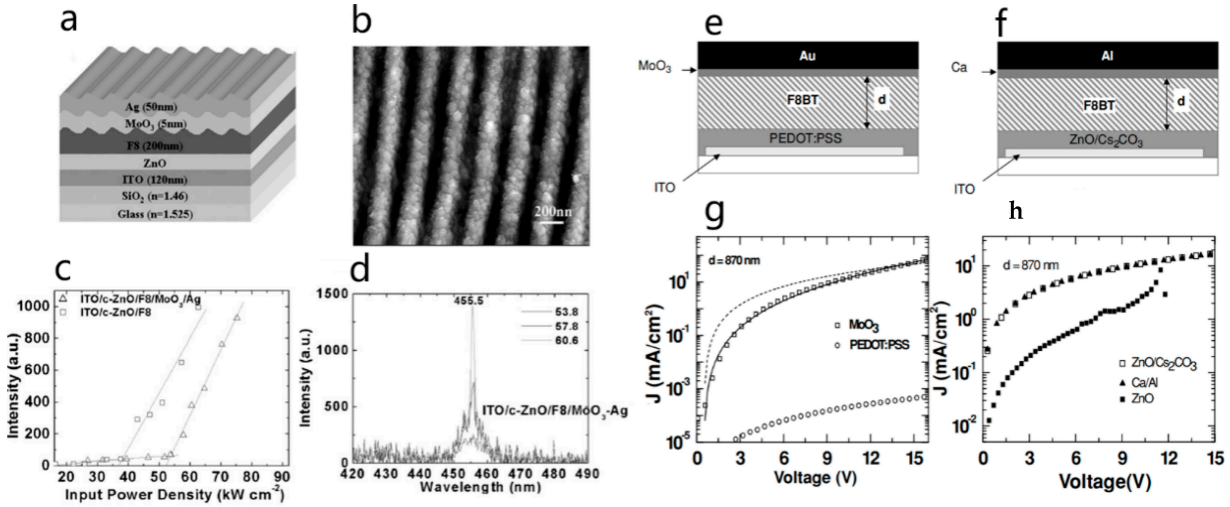


Figure 19. (**a**) Graphic depiction of COPLED structures for corrugated F8 films with ITO cathodes, ZnO electron injection layers, MoO_3 layers for hole injection, and silver anodes. (**b**) Tapping mode AFM micrograph of a polymer DFB laser diode composition with corrugations of 278 nm period and a depth of 40 nm. (**c**) Threshold performance in polymer DFB lasers fabricated with ITO/ZnO/F8 (E_{th} = 19.1 mJ cm^{-2} /$pulse^{-1}$; 38 kW cm^{-2}) and ITO/ZnO/F8/MoO_3/Ag (E_{th} = 27.1 mJ cm^{-2}/$pulse^{-1}$; 54 kW cm^{-2}), respectively. (**d**) A sequence of emission spectra right beneath (bottom line) and over the threshold (middle and top line) values for an ITO/ZnO/F8/MoO_3/Ag layout. (**a**–**d**) [105] Copyright 2009 Advanced Functional Materials (**e**) Illustration of hole-only devices (ITO/PEDOT:PSS/F8BT/MoO_3/Au). (**f**) Schematic of electron-only devices (ITO/ZnO/Cs_2CO_3/F8BT/Ca/Al). (**g**) J-V characteristics of hole-only devices for hole injection obtained from MoO_3 (white squares) as well as from PEDOT: PSS (white circles) for an F8BT thickness of 870 nm. (**h**) J-V characteristics of electron-only devices for electron injection from ZnO/Cs_2CO_3 (white squares), Ca/Al (black triangles), and ZnO (black squares) for F8BT thickness of 870 nm. (**e**–**h**) [106] Copyright 2010, Advanced Materials.

A more effective approach is to increase the separation between the electrode and the laser activation status in the cavity. For instance, Wallikewitz [100] increased the thickness of the charge transmission layer, fabricating the electrode further away from the laser mode, thus weakening the electrode absorption. Additionally, there are waveguides similar to the organic and inorganic hybrid designs mentioned earlier, where the gain media and the structure of the thick cavity transport layer are sandwiched, and the thickness of each layer is optimized to implement TE2 mode. In this mode, contact points are set at the nodes between the buffer layer and the core, allowing the aluminum-doped zinc oxide (azo) electrode layer to be inserted between the magnetic core and the buffer layer, significantly reducing the electrode loss [109]. Another innovative device, the light-emitting field-effect transistor (LEFET), combines light generation capabilities with the advantages of high carrier mobility from the field-effect transistor [100]. The LEFET possesses advantages that traditional OLEDs cannot match. When operating in a bipolar state, the holes and electrons in the LEFET are balanced, while the compound region is operated in the transistor channel and isolated from the metal electrode. Even in the presence of carrier imbalance, the distance between the metal electrode and the carrier composite zone exceeds 300 nm, leading to a significant reduction in the loss of the metal electrode and limiting the excitation threshold to a low level [110,111].

5.2.3. Polaronic Loss Reduction

In addition to the losses from the triple state and electrode, the carrier (dipole) itself also contributes significantly to the overall loss in the electrically pumped organic laser. The dipole has a wide absorption band, which covers the emitting band of the device and absorbs photons or quenches singlet states [96]. Rabe [112], using the hole-transporting material spiro-bifluorene, conducted precise dual measurements of the absorption cross-section. The results of his experiment confirmed that the dipole interaction mainly occurs between dipole-exciton quenching rather than direct photon absorption.

The presence of a dipole makes it challenging to maintain a high-level device carrier mobility. Generally, the carrier mobility of amorphous organic semiconductors falls in the range of 10^{-5} to 10^{-2} $cm^2 \cdot V^{-1} \cdot s^{-1}$. Achieving significant current densities in the devices requires a large number of dipole transports to occur [113]. To further obtain a large electric field in organic thin film devices with low carrier mobility, a small separation between two electrodes is required. In fact, both electrode and dipole generation losses result from the low carrier mobility characteristics of organic semiconductors. However, the organic light-emitting field-effect transistor (OLEFET) device structure has played a significant role in finding a solution to these problems. Firstly, the carrier mobility of the OLEFET is much higher than that of the OLED [114], and it has even achieved several $kA \cdot cm^{-2}$ current densities [115]. Additionally, in the OLEFET structure, the electrode is placed far away from the gain medium, which significantly reduces the exciton quenching of the electrode and minimizes electrode loss. By using OLEFET devices [11], accumulated carriers can be reassembled over long distances [44], significantly reducing the influence of dipoles, and keeping the losses at a low level [56].

Although the electrically pumped organic laser has not been realized in an OLEFET structure yet [95], its excellent performance in improving carrier mobility and reducing modal loss makes it the most promising organic laser diode structure [12]. It is believed that with in-depth investigations by researchers, the organic laser diode will eventually become a reality. Ultimately, the goal is to transition the organic laser diode from research laboratories to the production of practical devices in the industry [108].

6. Summary and Prospect

To summarize, we conducted a comprehensive analysis of the relevant factors affecting the threshold conditions of organic semiconductor laser devices. We explored measures to reduce the excitation threshold, taking into account both the positive and negative aspects of modal gain and modal loss [113].

Initially, we introduced the development of optically pumped organic laser devices, followed by a presentation of current research on gain materials and device structures. We also described methods to reduce modal loss, especially triplet loss, and construct high Q-value device structures. Additionally, we delved into the various bottlenecks encountered in electrically pumped organic laser devices. We further explored the application of material doping and the use of new structures, as well as raising carrier mobility and reducing triplet, electrode, and dipole losses to lower the excitation threshold. Another potential technique we discussed was the organic laser diode OLEFET structure [116].

Optically pumped OSSLs have found extensive applications in on-chip spectroscopy, optical communication technology, biomedicine, and low-cost sensing. Although the electrically pumped OLSD was not realized until 2023, theoretical analysis and experiments have made significant progress in stimulating gain media with low lasing thresholds, high gain, excellent stability, and high charge carrier mobility. The structure design has also been influenced by bionic design and sophisticated semiconductor structures. Ideas from the design and optimization of OLED light-emitting structures have provided valuable insights for OLSD. In the next decade, mature semiconductor structures, such as field-effect transistors, are expected to offer new guidelines for stability and efficiency.

We hope that continuous research and development, building upon the findings discussed in this paper and beyond, will make low-threshold and high-performance organic laser devices a reality in the future.

Funding: This project is financially supported by National Key R&D Plan (2021YFB4000901), National Natural Science Foundation of China (NSFC 62005035).

Institutional Review Board Statement: Not applicable.

Informed Consent Statement: Not applicable.

Data Availability Statement: Not applicable.

Conflicts of Interest: The authors declare no conflict of interest.

References

1. Schäfer, F.P.; Schmidt, W.; Volze, J. Organic Dye Solution Laser. *Appl. Phys. Lett.* **1966**, *9*, 306–309. [CrossRef]
2. Kuehne, A.J.C.; Gather, M.C. Organic Lasers: Recent Developments on Materials, Device Geometries, and Fabrication Techniques. *Chem. Rev.* **2016**, *116*, 12823–12864. [CrossRef] [PubMed]
3. Jiang, Y.; Liu, Y.-Y.; Liu, X.; Lin, H.; Gao, K.; Lai, W.-Y.; Huang, W. Organic solid-state lasers: A materials view and future development. *Chem. Soc. Rev.* **2020**, *49*, 5885–5944. [CrossRef] [PubMed]
4. Zhao, J.; Yan, Y.; Gao, Z.; Du, Y.; Dong, H.; Yao, J.; Zhao, Y.S. Full-color laser displays based on organic printed microlaser arrays. *Nat. Commun.* **2019**, *10*, 870. [CrossRef] [PubMed]
5. Gather, M.C.; Yun, S.H. Single-cell biological lasers. *Nat. Photonics* **2011**, *5*, 406–410. [CrossRef]
6. Balslev, S.; Bilenberg, B.; Geschke, O.; Jorgensen, A.M.; Kristensen, A.; Kutter, J.P.; Mogensen, K.B.; Snakenborg, D. Fully integrated optical systems for lab-on-a-chip applications. In Proceedings of the SPIE—The International Society for Optical Engineering, Maastricht, The Netherlands, 25–29 January 2004; Volume 5730, p. 7.
7. Zhou, Z.; Qiao, W.; Wang, Q.; Chenab, L.; Huang, W. Microfluidic channels incorporating organic distributed Bragg reflector lasers for in situ sensing applications. *J. Mater. Chem. C* **2018**, *6*, 2565–2572. [CrossRef]
8. Hide, F.; Díaz-García, M.A.; Schwartz, B.J.; Andersson, M.R.; Pei, Q.; Heeger, A.J. Semiconducting polymers: A new class of solid-state laser materials. *Science* **1996**, *273*, 1833–1836. [CrossRef]
9. Tessler, N.; Denton, G.J.; Friend, R.H. Lasing from conjugated-polymer microcavities. *Nature* **1996**, *382*, 695–697. [CrossRef]
10. Giebink, N.C.; Forrest, S.R. Temporal response of optically pumped organic semiconductor lasers and its implication for reaching threshold under electrical excitation. *Phys. Rev. B* **2009**, *79*, 073302. [CrossRef]
11. Yazdani, S.A.; Mikaeili, A.; Bencheikh, F.; Adachi, C. Impact of excitonic and photonic loss mechanisms on the threshold and slope efficiency of organic semiconductor lasers. *Jpn. J. Appl. Phys.* **2022**, *61*, 074003. [CrossRef]
12. Steer, R.P. Electronic energy pooling in organic systems: A cross-disciplinary tutorial review. *Can. J. Chem.* **2017**, *95*, 1025–1040. [CrossRef]
13. Kersting, R.; Lemmer, U.; Mahrt, R.F.; Leo, K.; Kurz, H.; Bässler, H.; Göbel, E.O. Femtosecond Energy Relaxation in Pi-Conjugated Polymers. *Phys. Rev. Lett.* **1993**, *70*, 3820–3823. [CrossRef] [PubMed]
14. Samuel, I.; Crystall, B.; Rumbles, G.; Burn, P.; Holmes, A.; Friend, R. Time-Resolved Luminescence Measurements in Poly(p-phenylenevinylene). *Synth. Met.* **1993**, *54*, 281–288. [CrossRef]
15. Kozlov, V.G.; Bulović, V.; Burrows, P.E.; Forrest, S.R. Laser action in organic semiconductor waveguide and double-heterostructure devices. *Nature* **1997**, *389*, 362–364. [CrossRef]
16. Rauscher, U.; Bässler, H.; Bradley, D.D.C.; Hennecke, M. Exciton Versus Band Description of the Absorption and Luminescence Spectra in Poly(Para-Phenylenevinylene). *Phys. Rev. B* **1990**, *42*, 9830–9836. [CrossRef] [PubMed]
17. Rudenko, A.I.; Bässler, H. Spectral Diffusion in Random Media: A Master Equation Approach. *Chem. Phys. Lett.* **1991**, *182*, 581–587. [CrossRef]
18. Brouwer, H.-J.; Krasnikov, V.V.; Hilberer, A.; Wildeman, J.; Hadziioannou, G. Novel High Efficiency Copolymer Laser Dye in the Blue Wavelength Region. *Appl. Phys. Lett.* **1995**, *66*, 3404–3406. [CrossRef]
19. Rabe, T.; Hoping, M.; Schneider, D.; Becker, E.; Johannes, H.-H.; Kowalsky, W.; Weimann, T.; Wang, J.; Hinze, P.; Nehls, B.S.; et al. Threshold reduction in polymer lasers based on poly(9,9-dioctylfluorene) with statistical binaphthyl units. *Adv. Funct. Mater.* **2005**, *15*, 1188–1192. [CrossRef]
20. Clark, J.; Lanzani, G. Organic photonics for communications. *Nat. Photonics* **2010**, *4*, 438–446. [CrossRef]
21. Cabanillas-Gonzalez, J.; Grancini, G.; Lanzani, G. Pump-Probe Spectroscopy in Organic Semiconductors: Monitoring Fundamental Processes of Relevance in Optoelectronics. *Adv. Mater.* **2011**, *23*, 5468–5485. [CrossRef] [PubMed]
22. Lehnhardt, M.; Riedl, T.; Weimann, T.; Kowalsky, W. Impact of triplet absorption and triplet-singlet annihilation on the dynamics of optically pumped organic solid-state lasers. *Phys. Rev. B* **2010**, *81*, 165206. [CrossRef]
23. Samuel, I.D.W.; Turnbull, G.A. Organic semiconductor lasers. *Chem. Rev.* **2007**, *107*, 1272–1295. [CrossRef]
24. Gritsai, Y.; Sakhno, O.; Goldenberg, L.M.; Stumpe, J. Dye-doped PQ-PMMA phase holographic materials for DFB lasing. *J. Opt.* **2014**, *16*, 035101. [CrossRef]

25. Ahmad, M.; King, T.A.; Ko, D.-K.; Cha, B.H.; Lee, J. Performance and photostability of xanthene and pyrromethene laser dyes in sol-gel phases. *J. Phys. D Appl. Phys.* **2002**, *35*, 1473–1476. [CrossRef]
26. Wallikewitz, B.H.; Nikiforov, G.O.; Sirringhaus, H.; Friend, R.H. A nanoimprinted, optically tuneable organic laser. *Appl. Phys. Lett.* **2012**, *100*, 173301. [CrossRef]
27. Liu, L.; Huang, W.; Diao, Z.; Peng, Z.; Mu, Q.Q.; Liu, Y.; Yang, C.; Hu, L.; Xuan, L. Low threshold of distributed feedback lasers based on scaffolding morphologic holographic polymer dispersed liquid crystal gratings: Reduced losses through Forster transfer. *Liq. Cryst.* **2014**, *41*, 145–152. [CrossRef]
28. Dogariu, A.; Gupta, R.; Heeger, A.J.; Wang, H. Time-resolved Förster energy transfer in polymer blends. *Synth. Met.* **1999**, *100*, 95–100. [CrossRef]
29. Sheridan, A.K.; Buckley, A.R.; Fox, A.M.; Bacher, A.; Bradley, D.D.C.; Samuel, I.D.W. Efficient energy transfer in organic thin films—Implications for organic lasers. *J. Appl. Phys.* **2002**, *92*, 6367–6371. [CrossRef]
30. Zhang, Y.; Forrest, S.R. Existence of continuous-wave threshold for organic semiconductor lasers. *Phys. Rev. B* **2011**, *84*, 241301. [CrossRef]
31. Ye, H.; Cui, L.-S.; Matsushima, T.; Qin, C.; Adachi, C. Deep-Red Amplified Spontaneous Emission from *cis*-Configured Squaraine. *ACS Appl. Mater. Interfaces* **2018**, *10*, 27–31. [CrossRef] [PubMed]
32. Tang, C.W.; Vanslyke, S.A. Organic electroluminescent diodes. *Appl. Phys. Lett.* **1987**, *51*, 913. [CrossRef]
33. Wu, C.; DeLong, M.; Vardeny, Z.; Ferraris, J. Structual and optical studies of distyrylbenzene single crystals. *Synth. Met.* **2003**, *137*, 939–941. [CrossRef]
34. Nakanotani; Adachi, C. Amplified Spontaneous Emission and Electroluminescence from Thiophene/Phenylene Co-Oligomer-Doped p-bis(p-Styrylstyryl)Benzene Crystals. *Adv. Opt. Mater.* **2013**, *1*, 422–427. [CrossRef]
35. Nakanotani, H.; Saito, M.; Nakamura, H.; Adachi, C. Highly balanced ambipolar mobilities with intense electroluminescence in field-effect transistors based on organic single crystal oligo(p-phenylenevinylene) derivatives. *Appl. Phys. Lett.* **2009**, *95*, 033308. [CrossRef]
36. Gierschner, J.; Park, S.Y. Luminescent distyrylbenzenes: Tailoring molecular structure and crystalline morphology. *J. Mater. Chem. C* **2013**, *1*, 5818–5832. [CrossRef]
37. Kabe, R.; Nakanotani, H.; Sakanoue, T.; Yahiro, M.; Adachi, C. Effect of Molecular Morphology on Amplified Spontaneous Emission of Bis-Styrylbenzene Derivatives. *Adv. Mater.* **2009**, *21*, 4034–4038. [CrossRef]
38. Ishow, E.; Brosseau, A.; Clavier, G.; Nakatani, K.; Tauc, P.; Fiorini-Debuisschert, C.; Neveu, S.; Sandre, O.; Léaustic, A. Multicolor Emission of Small Molecule-Based Amorphous Thin Films and Nanoparticles with a Single Excitation Wavelength. *Chem. Mater.* **2008**, *20*, 6597–6599. [CrossRef]
39. Rabbani-Haghighi, H.; Forget, S.; Chénais, S.; Siove, A.; Castex, M.-C.; Ishow, E. Laser operation in nondoped thin films made of a small-molecule organic red-emitter. *Appl. Phys. Lett.* **2009**, *95*, 033305. [CrossRef]
40. Forget, S.; Chenais, S.; Tondelier, D.; Geffroy, B.; Gozhyk, I.; Lebental, M.; Ishow, E. Red-emitting fluorescent organic light emitting diodes with low sensitivity to self-quenching. *J. Appl. Phys.* **2010**, *108*, 064509. [CrossRef]
41. Choi, E.Y.; Mazur, L.; Mager, L.; Gwon, M.; Pitrat, D.; Mulatier, J.C.; Monnereau, C.; Fort, A.; Attias, A.J.; Dorkenoo, K.; et al. Photophysical, amplified spontaneous emission and charge transport properties of oligofluorene derivatives in thin films. *Phys. Chem. Chem. Phys.* **2014**, *16*, 16941–16956. [CrossRef]
42. Sandanayaka, A.S.D.; Zhao, L.; Pitrat, D.; Mulatier, J.-C.; Matsushima, T.; Andraud, C.; Kim, J.-H.; Ribierre, J.-C.; Adachi, C. Improvement of the quasi-continuous-wave lasing properties in organic semiconductor lasers using oxygen as triplet quencher. *Appl. Phys. Lett.* **2016**, *108*, 223301. [CrossRef]
43. Nakanotani, H.; Akiyama, S.; Ohnishi, D.; Moriwake, M.; Yahiro, M.; Yoshihara, T.; Tobita, S.; Adachi, C. Extremely low-threshold amplified spontaneous emission of 9,9′-spirobifluorene derivatives and electroluminescence from field-effect transistor structure. *Adv. Funct. Mater.* **2007**, *17*, 2328–2335. [CrossRef]
44. Zhang, W.; Yan, Y.; Gu, J.; Yao, J.; Zhao, Y.S. Low-threshold wavelength-switchable organic nanowire lasers based on excited-state intramolecular proton transfer. *Angew. Chem. Int. Ed. Engl.* **2015**, *54*, 7125–7129. [CrossRef]
45. Tsiminis, G.; Montgomery, N.A.; Kanibolotsky, A.L.; Ruseckas, A.; Perepichka, I.F.; Skabara, P.J.; Turnbull, G.A.; Samuel, I.D.W. Laser characteristics of a family of benzene-cored star-shaped oligofluorenes. *Semicond. Sci. Technol.* **2012**, *27*, 94005. [CrossRef]
46. Guilhabert, B.; Laurand, N.; Herrnsdor, J.; Chen, Y.; Mackintosh, A.R.; Kanibolotsky, A.L.; Gu, E.; Skabara, P.J.; Pethrick, R.A.; Dawson, M.D. Amplified spontaneous emission in free-standing membranes incorporating star-shaped monodisperse pi-conjugated truxene oligomers. *J. Opt.* **2010**, *12*, 035503. [CrossRef]
47. Tsiminis, G.; Wang, Y.; Shaw, P.E.; Kanibolotsky, A.L.; Perepichka, I.F.; Dawson, M.D.; Skabara, P.J.; Turnbull, G.A.; Samuel, I.D.W. Low-threshold organic laser based on an oligofluorene truxene with low optical losses. *Appl. Phys. Lett.* **2009**, *94*, 243304. [CrossRef]
48. Ribierre, J.C.; Tsiminis, G.; Richardson, S.; Turnbull, G.A.; Samuel, I.D.W.; Barcena, H.S.; Burn, P.L. Amplified spontaneous emission and lasing properties of bisfluorene-cored dendrimers. *Appl. Phys. Lett.* **2007**, *91*, 081108. [CrossRef]
49. Lai, W.-Y.; Xia, R.; Bradley, D.D.C.; Huang, W. 2,3,7,8,12,13-Hexaaryltruxenes: An ortho-Substituted Multiarm Design and Microwave-Accelerated Synthesis toward Starburst Macromolecular Materials with Well-Defined pi Delocalization. *Chem. Eur. J.* **2010**, *16*, 8471–8479. [CrossRef] [PubMed]

50. Lai, W.-Y.; Xia, R.; He, Q.; Levermore, P.A.; Huang, W.; Bradley, D.D.C. Enhanced Solid-State Luminescence and Low-Threshold Lasing from Starburst Macromolecular Materials. *Adv. Mater.* **2009**, *21*, 355–360. [CrossRef]
51. Chen, S.; Kwok, H.-S. Alleviate microcavity effects in top-emitting white organic light-emitting diodes for achieving broadband and high color rendition emission spectra. *Org. Electron.* **2011**, *12*, 2065–2070. [CrossRef]
52. Yap, B.K.; Xia, R.; Campoy-Quiles, M.; Stavrinou, P.N.; Bradley, D.D.C. Simultaneous optimization of charge-carrier mobility and optical gain in semiconducting polymer films. *Nat. Mater.* **2008**, *7*, 376–380. [CrossRef]
53. Stavrinou, P.N.; Ryu, G.; Campoy-Quiles, M.; Bradley, D.D.C. The change in refractive index of poly(9,9-dioctylfluorene) due to the adoption of the beta-phase chain conformation. *J. Phys. Condens. Matter* **2007**, *19*, 466107. [CrossRef]
54. Xia, R.; Campoy-Quiles, M.; Heliotis, G.; Stavrinou, P.; Whitehead, K.S.; Bradley, D.D. Significant improvements in the optical gain properties of oriented liquid crystalline conjugated polymer films. *Synth. Met.* **2005**, *155*, 274–278. [CrossRef]
55. Lin, J.-Y.; Zhu, W.-S.; Liu, F.; Xie, L.-H.; Zhang, L.; Xia, R.; Xing, G.-C.; Huang, W. A Rational Molecular Design of beta-Phase Polydiarylfluorenes: Synthesis, Morphology, and Organic Lasers. *Macromolecules* **2014**, *47*, 1001–1007. [CrossRef]
56. Zhang, B.; Pinky, S.K.; Kwansa, A.L.; Ferguson, S.; Yingling, Y.G.; Stiff-Roberts, A.D. Correlation of Emulsion Chemistry, Film Morphology, and Device Performance in Polyfluorene LEDs Deposited by RIR-MAPLE. *ACS Appl. Mater. Interfaces* **2023**, *15*, 18153–18165. [CrossRef] [PubMed]
57. Kuehne, A.J.C.; Kaiser, M.; Mackintosh, A.R.; Wallikewitz, B.H.; Hertel, D.; Pethrick, R.A.; Meerholz, K. Sub-Micrometer Patterning of Amorphous- and beta-Phase in a Crosslinkable Poly(9,9-dioctylfluorene): Dual-Wavelength Lasing from a Mixed-Morphology Device. *Adv. Funct. Mater.* **2011**, *21*, 2564–2570. [CrossRef]
58. Kallinger, C.; Hilmer, M.; Haugeneder, A.; Perner, M.; Spirkl, W.; Lemmer, U.; Feldmann, J.; Scherf, U.; Müllen, K.; Gombert, A.; et al. A flexible conjugated polymer laser. *Adv. Mater.* **1998**, *10*, 920–923. [CrossRef]
59. Xia, R.; Heliotis, G.; Bradley, D.D.C. Fluorene-based polymer gain media for solid-state laser emission across the full visible spectrum. *Appl. Phys. Lett.* **2003**, *82*, 3599–3601. [CrossRef]
60. Xia, R.; Stavrinou, P.N.; Bradley, D.D.C.; Kim, Y. Efficient optical gain media comprising binary blends of poly(3-hexylthiophene) and poly(9,9-dioctylfluorene-*co*-benzothiadiazole). *J. Appl. Phys.* **2012**, *111*, 123107. [CrossRef]
61. Qin, C.; Sandanayaka, A.S.D.; Zhao, C.; Matsushima, T.; Zhang, D.; Fujihara, T.; Adachi, C. Stable room-temperature continuous-wave lasing in quasi-2D perovskite films. *Nature* **2020**, *585*, 53–57. [CrossRef]
62. Veldhuis, S.A.; Boix, P.P.; Yantara, N.; Li, M.; Sum, T.C.; Mathews, N.; Mhaisalkar, S.G. Perovskite Materials for Light-Emitting Diodes and Lasers. *Adv. Mater.* **2016**, *28*, 6804–6834. [CrossRef] [PubMed]
63. Stranks, S.D.; Wood, S.M.; Wojciechowski, K.; Deschler, F.; Saliba, M.; Khandelwal, H.; Patel, J.B.; Elston, S.J.; Herz, L.M.; Johnston, M.B.; et al. Enhanced Amplified Spontaneous Emission in Perovskites Using a Flexible Cholesteric Liquid Crystal Reflector. *Nano Lett.* **2015**, *15*, 4935–4941. [CrossRef] [PubMed]
64. Xing, G.; Mathews, N.; Lim, S.S.; Yantara, N.; Liu, X.; Sabba, D.; Grätzel, M.; Mhaisalkar, S.; Sum, T.C. Low-temperature solution-processed wavelength-tunable perovskites for lasing. *Nat. Mater.* **2014**, *13*, 476–480. [CrossRef] [PubMed]
65. Hung, Y.-C.; Su, C.-H.; Huang, H.-W. Low threshold amplified spontaneous emission from dye-doped DNA biopolymer. *J. Appl. Phys.* **2012**, *111*, 113107. [CrossRef]
66. Ramos-Ortiz, G.; Spiegelberg, C.; Peyghambarian, N.; Kippelen, B. Temperature dependence of the threshold for laser emission in polymer microlasers. *Appl. Phys. Lett.* **2000**, *77*, 2783–2785. [CrossRef]
67. Rotschild, C.; Tomes, M.; Mendoza, H.; Andrew, T.L.; Swager, T.M.; Carmon, T.; Baldo, M.A. Cascaded Energy Transfer for Efficient Broad-Band Pumping of High-Quality, Micro-Lasers. *Adv. Mater.* **2011**, *23*, 3057–3060. [CrossRef] [PubMed]
68. He, L.; Özdemir, K.; Yang, L. Whispering gallery microcavity lasers. *Laser Photonics Rev.* **2012**, *7*, 60–82. [CrossRef]
69. Grossmann, T.; Schleede, S.; Hauser, M.; Christiansen, M.B.; Vannahme, C.; Eschenbaum, C.; Klinkhammer, S.; Beck, T.; Fuchs, J.; Nienhaus, G.U.; et al. Low-threshold conical microcavity dye lasers. *Appl. Phys. Lett.* **2010**, *97*, 063304. [CrossRef]
70. Gather, M.C.; Yun, S.H. Bio-optimized energy transfer in densely packed fluorescent protein enables near-maximal luminescence and solid-state lasers. *Nat. Commun.* **2014**, *5*, 5722. [CrossRef]
71. Canazza, G.; Scotognella, F.; Lanzani, G.; De Silvestri, S.; Zavelani-Rossi, M.; Comoretto, D. Lasing from all-polymer microcavities. *Laser Phys. Lett.* **2014**, *11*, 035804. [CrossRef]
72. Kogelnik, H.; Shank, C.V. Coupled-Wave Theory of Distributed Feedback Lasers. *J. Appl. Phys.* **1972**, *43*, 2327–2335. [CrossRef]
73. Holzer, W.; Penzkofer, A.; Pertsch, T.; Danz, N.; Bräuer, A.; Kley, E.; Tillmann, H.; Bader, C.; Hörhold, H.-H. Corrugated neat thin-film conjugated polymer distributed-feedback lasers. *Appl. Phys. B Laser Opt.* **2002**, *74*, 333–342. [CrossRef]
74. Rose, A.; Zhu, Z.; Madigan, C.F.; Swager, T.M.; Bulović, V. Sensitivity gains in chemosensing by lasing action in organic polymers. *Nature* **2005**, *434*, 876–879. [CrossRef]
75. Karnutsch, C.; Pflumm, C.; Heliotis, G.; Demello, J.C.; Bradley, D.D.C.; Wang, J.; Weimann, T.; Haug, V.; Gärtner, C.; Lemmer, U. Improved organic semiconductor lasers based on a mixed-order distributed feedback resonator design. *Appl. Phys. Lett.* **2007**, *90*, 131104. [CrossRef]
76. Karnutsch, C.; Gýrtner, C.; Haug, V.; Lemmer, U.; Farrell, T.; Nehls, B.S.; Scherf, U.; Wang, J.; Weimann, T.; Heliotis, G.; et al. Low threshold blue conjugated polymer lasers with first- and second-order distributed feedback. *Appl. Phys. Lett.* **2006**, *89*, 201108. [CrossRef]
77. Schneider, D.; Rabe, T.; Riedl, T.; Dobbertin, T.; Kröger, M.; Becker, E.; Johannes, H.-H.; Kowalsky, W.; Weimann, T.; Wang, J.; et al. Ultrawide tuning range in doped organic solid-state lasers. *Appl. Phys. Lett.* **2004**, *85*, 1886–1888. [CrossRef]

78. Goossens, M.; Ruseckas, A.; Turnbull, G.A.; Samuel, I.D.W. Subpicosecond pulses from a gain-switched polymer distributed feedback laser. *Appl. Phys. Lett.* **2004**, *85*, 31–33. [CrossRef]
79. Heliotis, G.; Xia, R.; Turnbull, G.A.; Andrew, P.; Barnes, W.L.; Samuel, I.D.W.; Bradley, D.D.C. Emission characteristics and performance comparison of polyfluorene lasers with one- and two-dimensional distributed feedback. *Adv. Funct. Mater.* **2004**, *14*, 91–97. [CrossRef]
80. Forberich, K.; Diem, M.; Crewett, J.; Lemmer, U.; Gombert, A.; Busch, K. Lasing action in two-dimensional organic photonic crystal lasers with hexagonal symmetry. *Appl. Phys. B Laser Opt.* **2006**, *82*, 539–541. [CrossRef]
81. Notomi, M.; Suzuki, H.; Tamamura, T. Directional lasing oscillation of two-dimensional organic photonic crystal lasers at several photonic band gaps. *Appl. Phys. Lett.* **2001**, *78*, 1325–1327. [CrossRef]
82. Dodabalapur, A.; Berggren, M.; Slusher, R.; Bao, Z.; Timko, A.; Schiortino, P.; Laskowski, E.; Katz, H.; Nalamasu, O. Resonators and materials for organic lasers based on energy transfer. *IEEE J. Sel. Top. Quantum Electron.* **1998**, *4*, 67–74. [CrossRef]
83. Turnbull, G.A.; Andrew, P.; Barnes, W.L.; Samuel, I.D.W. Operating characteristics of a semiconducting polymer laser pumped by a microchip laser. *Appl. Phys. Lett.* **2003**, *82*, 313–315. [CrossRef]
84. Senevirathne, C.A.M.; Sandanayaka, A.S.D.; Karunathilaka, B.S.B.; Fujihara, T.; Bencheikh, F.; Qin, C.; Goushi, K.; Matsushima, T.; Adachi, C. Markedly Improved Performance of Optically Pumped Organic Lasers with Two-Dimensional Distributed-Feedback Gratings. *ACS Photonics* **2021**, *8*, 1324–1334. [CrossRef]
85. Grudinin, I.S.; Ilchenko, V.S.; Maleki, L. Ultrahigh optical Q factors of crystalline resonators in the linear regime. *Phys. Rev. A* **2006**, *74*, 063806. [CrossRef]
86. Wienhold, T.; Kraemmer, S.; Wondimu, S.F.; Siegle, T.; Bog, U.; Weinzierl, U.; Schmidt, S.; Becker, H.; Kalt, H.; Mappes, T.; et al. All-polymer photonic sensing platform based on whispering-gallery mode microgoblet lasers. *Lab Chip* **2015**, *15*, 3800–3806. [CrossRef]
87. Baktur, R.; Pearson, L.W.; Ballato, J. Theoretical determination of lasing resonances in a microring. *J. Appl. Phys.* **2007**, *101*, 043102. [CrossRef]
88. Mizuno, H.; Haku, U.; Marutani, Y.; Ishizumi, A.; Yanagi, H.; Sasaki, F.; Hotta, S. Single Crystals of 5,5′-Bis(4′-methoxybiphenyl-4-yl)-2,2′-bithiophene for Organic Laser Media. *Adv. Mater.* **2012**, *24*, 5744–5749. [CrossRef]
89. Xu, Z.; Liao, Q.; Shi, Q.; Zhang, H.; Yao, J.; Fu, H. Low-Threshold Nanolasers Based on Slab-Nanocrystals of H-Aggregated Organic Semiconductors. *Adv. Mater.* **2012**, *24*, OP216–OP220. [CrossRef]
90. Dhayal, R.S.; Liao, J.-H.; Liu, Y.-C.; Chiang, M.-H.; Kahlal, S.; Saillard, J.-Y.; Liu, C.W. $[Ag_{21}\{S_2P(OiPr)_2\}_{12}]^+$: An Eight-Electron Superatom. *Angew. Chem. Int. Ed.* **2015**, *54*, 3702–3706. [CrossRef]
91. Wang, X.; Liao, Q.; Kong, Q.; Zhang, Y.; Xu, Z.; Lu, X.; Fu, H. Whispering-Gallery-Mode Microlaser Based on Self-Assembled Organic Single-Crystalline Hexagonal Microdisks. *Angew. Chem. Int. Ed.* **2014**, *53*, 5863–5867. [CrossRef]
92. Wang, X.; Liao, Q.; Lu, X.; Li, H.; Xu, Z.; Fu, H. Shape-Engineering of Self-Assembled Organic Single Microcrystal as Optical Microresonator for laser Applications. *Sci. Rep.* **2014**, *4*, 7011. [CrossRef]
93. Camposeo, A.; Di Benedetto, F.; Stabile, R.; Neves, A.A.R.; Cingolani, R.; Pisignano, D. Laser Emission from Electrospun Polymer Nanofibers. *Small* **2009**, *5*, 562–566. [CrossRef]
94. Di Benedetto, F.; Camposeo, A.; Pagliara, S.; Mele, E.; Persano, L.; Stabile, R.; Cingolani, R.; Pisignano, D. Patterning of light-emitting conjugated polymer nanofibres. *Nat. Nanotechnol.* **2008**, *3*, 614–619. [CrossRef]
95. Calzado, E.M.; Villalvilla, J.M.; Boj, P.G.; Quintana, J.A.; Díaz-García, M.A. Tuneability of amplified spontaneous emission through control of the thickness in organic-based waveguides. *J. Appl. Phys.* **2005**, *97*, 093103. [CrossRef]
96. Baldo, M.A.; Holmes, R.J.; Forrest, S.R. Prospects for electrically pumped organic lasers. *Phys. Rev. B* **2002**, *66*, 035321. [CrossRef]
97. Tessler, N.; Pinner, D.; Friend, R. Semiconductor device model applied to electrically pulsed polymer LEDs. *Synth. Met.* **2000**, *111–112*, 269–272. [CrossRef]
98. Sun, Y.; Borek, C.; Hanson, K.; Djurovich, P.I.; Thompson, M.E.; Brooks, J.; Brown, J.J.; Forrest, S.R. Photophysics of Pt-porphyrin electrophosphorescent devices emitting in the near infrared. *Appl. Phys. Lett.* **2007**, *90*, 213503. [CrossRef]
99. Susdorf, T.; Álvarez, M.; Holzer, W.; Penzkofer, A.; Amat-Guerri, F.; Liras, M.; Costela, A.; García-Moreno, I.; Sastre, R. Photophysical characterisation of some dipyrromethene dyes in ethyl acetate and covalently bound to poly(methyl methacrylate). *Chem. Phys.* **2005**, *312*, 151–158. [CrossRef]
100. Wallikewitz, B.H.; de la Rosa, M.; Kremer, J.H.-W.; Hertel, D.; Meerholz, K. A Lasing Organic Light-Emitting Diode. *Adv. Mater.* **2010**, *22*, 531–534. [CrossRef]
101. Sandanayaka, A.S.D.; Matsushima, T.; Bencheikh, F.; Terakawa, S.; Potscavage, W.J.P., Jr.; Qin, C.; Fujihara, T.; Goushi, K.; Ribierre, J.-C.; Adachi, C. Indication of current-injection lasing from an organic semiconductor. *Appl. Phys. Express* **2019**, *12*, 061010. [CrossRef]
102. Kozlov, V.; Parthasarathy, G.; Burrows, P.; Khalfin, V.; Wang, J.; Chou, S.; Forrest, S. Structures for organic diode lasers and optical properties of organic semiconductors under intense optical and electrical excitations. *IEEE J. Quantum Electron.* **2000**, *36*, 18–26. [CrossRef]
103. McGehee, M.D.; Heeger, A.J. Semiconducting (conjugated) polymers as materials for solid-state lasers. *Adv. Mater.* **2000**, *12*, 1655–1668. [CrossRef]
104. Tessler, N.; Harrison, N.T.; Friend, R.H. High peak brightness polymer light-emitting diodes. *Adv. Mater.* **1998**, *10*, 64–68. [CrossRef]

105. Song, M.H.; Kabra, D.; Wenger, B.; Friend, R.H.; Snaith, H.J. Optically-Pumped Lasing in Hybrid Organic-Inorganic Light-Emitting Diodes. *Adv. Funct. Mater.* **2009**, *19*, 2130–2136. [CrossRef]
106. Kabra, D.; Lu, L.P.; Song, M.H.; Snaith, H.J.; Friend, R.H. Efficient Single-Layer Polymer Light-Emitting Diodes. *Adv. Mater.* **2010**, *22*, 3194–3198. [CrossRef]
107. Lattante, S.; Romano, F.; Caricato, A.P.; Martino, M.; Anni, M. Low electrode induced optical losses in organic active single layer polyfluorene waveguides with two indium tin oxide electrodes deposited by pulsed laser deposition. *Appl. Phys. Lett.* **2006**, *89*, 031108. [CrossRef]
108. Gong, Q.X.; Zhang, W.; He, J.; Ma, F.; Song, L.; Cheng, L.; Zhang, J.; Wang, L.; Hu, Y. Simultaneously improving the quality factor and outcoupling efficiency of organic light-emitting field-effect transis-tors with planar microcavity. *Opt. Express* **2023**, *31*, 2480–2491. [CrossRef]
109. Görrn, P.; Rabe, T.; Riedl, T.; Kowalsky, W. Loss reduction in fully contacted organic laser waveguides using TE2 modes. *Appl. Phys. Lett.* **2007**, *91*, 041113. [CrossRef]
110. Capelli, R.; Toffanin, S.; Generali, G.; Usta, H.; Facchetti, A.; Muccini, M. Organic light-emitting transistors with an efficiency that outperforms the equivalent light-emitting diodes. *Nat. Mater.* **2010**, *9*, 496–503. [CrossRef]
111. Liu, J.; Zhang, H.; Dong, H.; Meng, L.; Jiang, L.; Jiang, L.; Wang, Y.; Yu, J.; Sun, Y.; Hu, W.; et al. High mobility emissive organic semiconductor. *Nat. Commun.* **2015**, *6*, 10032. [CrossRef]
112. Rabe, T.; Görrn, P.; Lehnhardt, M.; Tilgner, M.; Riedl, T.; Kowalsky, W. Highly Sensitive Determination of the Polaron-Induced Optical Absorption of Organic Charge-Transport Materials. *Phys. Rev. Lett.* **2009**, *102*, 137401. [CrossRef] [PubMed]
113. Samsonas, D.; Skliutas, E.; Čiburys, A.; Kontenis, L.; Gailevičius, D.; Berzinš, J.; Narbutis, D.; Jukna, V.; Vengris, M.; Juodkazis, S.; et al. 3D nanopolymerization and damage threshold dependence on laser wavelength and pulse duration. *Nanophotonics* **2023**, *12*, 1537–1548. [CrossRef]
114. Tanase, C.; Meijer, E.J.; Blom, P.W.M.; de Leeuw, D.M. Unification of the hole transport in polymeric field-effect transistors and light-emitting diodes. *Phys. Rev. Lett.* **2003**, *91*, 216601. [CrossRef]
115. Namdas, E.B.; Ledochowitsch, P.; Yuen, J.D.; Moses, D.; Heeger, A.J. High performance light emitting transistors. *Appl. Phys. Lett.* **2008**, *92*, 183304. [CrossRef]
116. Diroll, B.T.; Guzelturk, B.; Po, H.; Dabard, C.; Fu, N.; Makke, L.; Lhuillier, E.; Ithurria, S. 2D II–VI Semiconductor Nanoplatelets: From Material Synthesis to Optoelectronic Integration. *Chem. Rev.* **2023**, *123*, 3543–3624. [CrossRef] [PubMed]

Disclaimer/Publisher's Note: The statements, opinions and data contained in all publications are solely those of the individual author(s) and contributor(s) and not of MDPI and/or the editor(s). MDPI and/or the editor(s) disclaim responsibility for any injury to people or property resulting from any ideas, methods, instructions or products referred to in the content.